Research on Direct Shear Strength Characteristics of Mechanically Biologically Treated Waste

Zhenying Zhang (zhangzhenyinga@163.com)
Zhejiang Sci-Tech University https://orcid.org/0000-0002-4076-1926
Jiahe Zhang
Zhejiang Sci-Tech University
Qiaona Wang
Zhejiang Sci-Tech University
Min Wang
Zhejiang Sci-Tech University
Chengyu Nie
Zhejiang Sci-Tech University

Research Article

Keywords: Mechanically biologically treated municipal solid waste, Shearing displacement rate, landfill depth, shear strength, Shear strength characteristics, Shear strength model

Posted Date: March 9th, 2021

DOI: https://doi.org/10.21203/rs.3.rs-207864/v1

Research on Direct Shear Strength Characteristics of Mechanically biologically treated Waste

Zhenying Zhang[a,*], Jiahe Zhang[a], Qiaona Wang[a], Min Wang[a], Chengyu Nie[a]

[a]School of Civil Engineering and Architecture, Zhejiang Sci-Tech University, Hangzhou 310018, China

[*]Correspondence should be addressed to Zhenying Zhang; zhangzhenyinga@163.com

Abstract: Mechanically biologically treated (MBT) waste has significant characteristics such as high stability and low moisture content, which can reduce water, soil, and gas pollution in subsequent treatments. This pre-treatment method is environmentally friendly and sustainable, and has become a popular research topic in the field of environmental geotechnical engineering. Using a direct shear test apparatus and five shearing rates (0.25, 1, 5, 10, and 20 mm/min), the shear strength characteristics of MBT waste at the Hangzhou Tianziling (HT) Landfill were studied. The results indicate: (1). With the increase in horizontal shear displacement, the shear stress of MBT waste gradually increases without a peak stress phenomenon, which is a displacement hardening curve; (2). The shear strength increased with an increase in the shearing displacement rate, and the sensitivity coefficient was 0.64–2.66. (3). The

shear strength, shearing rate, and normal stress correlation model are established, and the model has a high degree of fit with the overall experimental data; (4). Cohesion (c), internal friction angle (φ), and the logarithm of the shearing rate are linear; (5). The range of c of MBT waste is 22.32–39.51 kPa, and φ is 64.24–.68.52°. Meanwhile, the test data are compared with the test data in the literature, and the shear characteristics of HT-MBT waste are discussed. The research results of this study can provide a reference for the stability calculation of MBT landfills.

Keywords: Mechanically biologically treated municipal solid waste, Shearing displacement rate, landfill depth, shear strength, Shear strength characteristics, Shear strength model

1. Introduction

Increasing population and rapid urbanisation have consequently led to an increase in the output of municipal solid waste (MSW) (Guerrero et al. 2013, Eskandari et al. 2016). Due to the vast amount of solid waste produced, pre-treatment processes for solid waste have gradually attracted attention. In April 1999, the European Union Landfill Directive (99/31/EC) defined the design and operation standards of landfills and mandatory requirements to reduce the biodegradable materials in MSW entering landfills. Under this directive, member states adopt different strategies to transfer organic matter in domestic waste from landfills, such as converting the biodegradable

41 component into fertiliser, incinerating MSW, and then proceeding with landfilling or
42 recycling the residue from incineration. Member states have also increased their focus
43 on pre-treatment technologies for untreated MSW, with mechanically biologically
44 treated (MBT) waste demonstrating the most favourable characteristics.

45 MBT technology is primarily divided into two parts: first, mechanical
46 processing (crushing, sieving, centrifugation, or selection) is used for separation of
47 biodegradable and non-biodegradable materials and large-size materials are sieved or
48 shredded. Next, biological treatment (anaerobic digestion and leaching hydrolysis,
49 etc.) accelerates the degradation of biomass in MSW. Compared with MSW that is
50 directly landfilled, MBT reduces the amount of biodegradable materials and their
51 biodegradability, thereby reducing environmental pollution caused by the discharge of
52 leachate and greenhouse gases. Therefore, this technology is applied in many
53 European cities (Kuehle-Weidemeier 2004). In several cases, the residue produced by
54 MBT does not have a high enough economic value making it unsuitable for use or a
55 disposal method other than landfill (Archer et al. 2005). However, because MBT
56 converts MSW into another material, the product from this pre-treatment varies from
57 its parent material in terms of characteristics. Thus, the physical properties of MSW
58 (particle size, composition, moisture content, density, and void ratio) to be discarded
59 in landfills are fundamentally changed (Zhang et al. 2018a), consequently changing its
60 mechanical properties, such as shear strength, compression, and consolidation. This

61 greatly affects the strength, stiffness, and stability of the landfill (Jones & Dixon,
62 2015). The design of the slope and pile stability calculation of the MBT landfill site
63 should be based on its mechanical characteristics to ensure the safety of the project.

64 Many researchers (Landva and Clark 1990, Singh and Murphy 1990, Kavazanjian
65 et al. 1995, Gabr and Valero 1995, Manassero et al. 1996, Jones et al. 1997, Machado
66 et al. 2002, Stark et al. 2009, Bray et al. 2009, Reddy et al. 2009a, Bareither et al.
67 2012, Zhang et al. 2014, Zhang et al. 2015, Zekkos and Fei 2016, Abreu and Vilar
68 2017, Fei and Zekkos 2017, Karimpour-Fard 2018, Falamaki et al. 2019, Keramati et
69 al. 2020) conducted a shear strength test study on MSW, and conducted an instability
70 failure simulation model analysis on an existing landfill. However, unlike MSW,
71 research on the shear strength of MBT waste appears to be more limited. Fucale
72 (2005), Mahler & Neto (2006), and Fucale et al. (2007) used direct shear (DS)
73 equipment to analyse the influence of fibre on the strength of MBT waste. Fucale
74 (2005) mixed MSW and MBT waste with different percentages of fibres to study the
75 effect of randomly distributed plastic fibres on the mechanical properties of the
76 material, and to verify the possible similarities between these properties. Mahler &
77 Neto (2006) observed that the fibre composition of MBT waste has a substantial
78 influence on the shear strength of MBT waste. This is because, although MBT waste
79 is characterised by a coarse material with non-sticky particle behaviour, it is due to the
80 tensile strength of the fibre is high; it may still show a high false viscosity value.

Fernando et al. (2009) and Fernando and Sudarshana (2011) conducted DS experiments on MBT waste with different reinforcement contents and compared the strength of MSW. Experimental results show that MBT waste is stronger than MSW. Petrovic and Bauer (2011) conducted experimental research and numerical simulations on the mechanical behaviour of MBT waste with different moisture contents. Bhandari and Powrie (2013) conducted triaxial experiments on MBT waste with different particle sizes and shapes to study the stress-strain-strength characteristics of MBT waste. Pimolthai and Wagner (2014) used DS equipment to test the shear strength of MBT waste with a particle size of less than 10 mm. Babu et al. (2015) used the DS test, and small-scale triaxial text and large-scale triaxial text apparatus were used for experiments to comprehensively test the shear strength characteristics of MBT waste. Fucale et al. (2015) experimentally found that the reinforcement phases (plastics, textiles, fibres, etc.) present in landfills have a great influence on the various characteristics (including strength) of MBT waste. Relevant literature on the shear strength characteristics of MBT waste is presented in Table 1.

Table 1. Reference summary.

Reference	Country	Testing method and sample size (mm)	Displacement or strain at the shearing resistance considered and vertical pressure (kPa)	c (kPa)	φ (°)

Fucale (2005)	Germany	L-DS, 100×100×30	PD (18mm), 100-300	18.7	10.2
Mahler and Neto (2006)	Brazil	L-DS, NA	PD (12mm), 25-100	NA	NA
Fernando et al. (2009)	United Kingdom	L-DS, NA	PD (4%), 100	NA	NA
			PD (3%), 50	NA	NA
Fernando (2011)	United Kingdom	L-DS, NA	NA	NA	NA
Petrovic and Bauer (2011)	Croatia	L-DS, NA	PD (NA), 36-180	NA	31-50
Bhandari and Powrie (2013)	NA	L-TT, NA	PD (35%), 25-200	NA	NA
Pimolthai and Wagner (2014)	Luxembourg	L-DS, 94(D) and 20(H)	PS, 20-100	12.8	36.5
	Germany			9.0	38.6
	Thailand			5.4	31.9
Babu et al. (2015)	India	L-DS, 60×60×30	PD(20%), 50-150	12	40
Fucale et al. (2015)	Switzerland	L-DS, 100×100×150	PD (20%), 100-300	16.0	40.1
				34.7	45.4
				63.1	48.1

L laboratory tests, DS direct shear, TT trixial text, PS peak stress, PD peak displacement, NA not available.

Few studies exist on the relationship between MBT waste at different shearing rates, landfill depths, and shear strength. This study considers the shearing rate, simulated landfill depth, and other factors, and systematically studies MBT shear strength characteristics. The theoretical model of shear strength prediction is established, and the variation range of the shear strength parameters is obtained. The findings of this work provide basic data and strength models for the design and

instability and destruction prediction of MBT landfills.

2. Materials, device, and process

2.1 Materials

Hangzhou is the largest city in Zhejiang province with a population of approximately 10.36 million. At least 12,000 t of domestic waste are generated daily, and part of the waste is transported to the Hangzhou Tianziling (HT) Landfill. The HT-MSW Treatment Plant is divided into two parts: the first (closed) and second (in operation) landfills. The second landfill is expanded vertically and horizontally on a one-field basis. Its total storage capacity is 22.02 million m^3, which can absorb 24.05 million t of MSW and treat 1,940–4,000 t of waste daily. The geographical location of the HTL is shown in Figure 1.

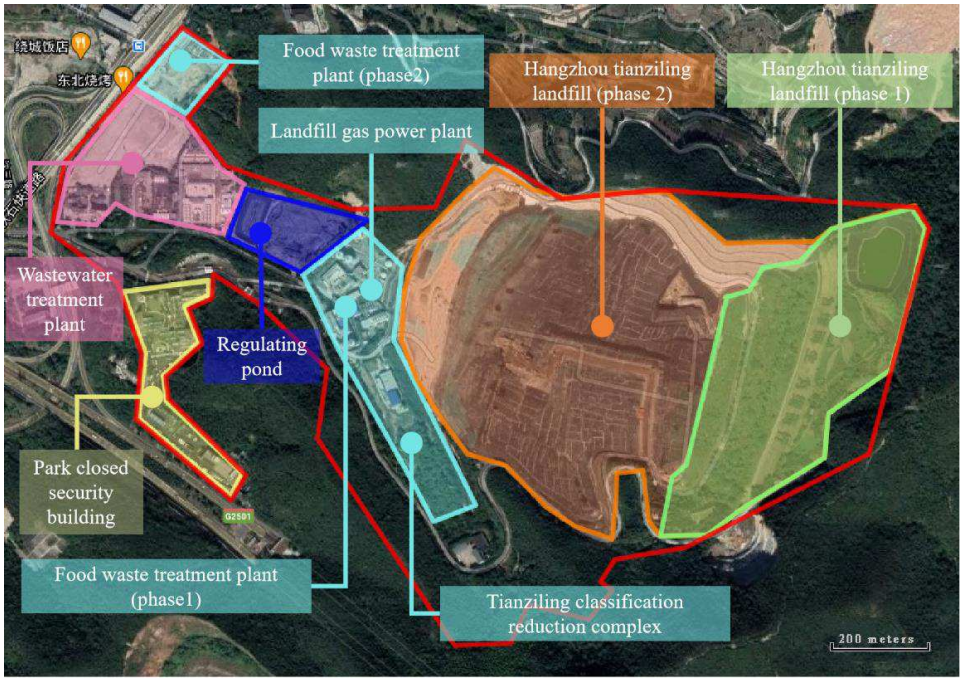

Figure 1 Floor plan of Hangzhou Tianziling Landfill, China.

The China Hangzhou Environment Group introduced MBT technology from Germany and produced MBT waste through several processes. First, the fresh MSW is crushed and sieved in a rotating drum screen with an aperture of 120 mm. Through the screen, large-sized materials (mainly cardboard, plastic, and textiles) are manually screened for recycling. The metal and material passing through the screen are separated by a magnetic separation method, and the remaining small-sized materials enter the reactor for hydrolysis treatment. Subsequently, the solid-phase hydrolysate with a moisture content of more than 40% is usually transferred to a drying chamber for biological drying. After biological drying for ~9 d, it eventually becomes MBT

132 waste. The test materials were obtained from the MBT factory, placed in sealed plastic
133 drums, and directly transported to the Environmental Geotechnical Materials
134 Laboratory of Zhejiang Sci-Tech University. The original appearance of the MBT
135 materials is shown in Figure 2.
136

137
138 Figure 2 MBT waste original materials.
139
140 The components and physical characteristics of HT-MBT waste are presented in
141 Table 2, which shows that MBT waste includes paper, plastic, rubber, textiles, wood,
142 stone, ceramics, glass, metal, fine-grained soil, and other visually indistinguishable
143 materials. Judging from the MBT waste, the most important components in MBT
144 waste are plastic and rubber, and their combined mass is 1,216.5 g, accounting for
145 23.3% of the total dry mass. This is because they are not easily biodegradable and

there is poor national recycling awareness. The quantity of the paper is 0 g, mainly because the paper is broken during the MBT process. After degradation, it is not the correct size of paper or easy to identify. The residue is classified into an undefined particle size. The moisture content of general waste is 60–80% (Gao et al. 2015), and the moisture content of MBT waste is 20%, which is significantly lower than that of general waste.

Table 2 Composition and physical properties of MBT waste sample

Composition (percentage by dry weight/g)									Specific gravity	Moisture content (%)
Paper	Plastic & rubber	Textile	Wood	Stones & ceramics	Glass	Metal	Undefined > 5mm	Fines <5mm		
0	1216.5	255.4	240.2	737.5	1076	139	465.9	1080.2	1.53	20.0

2.2 Direct shear test device

In this study, a DS apparatus (Figure 3) was used. This device uses a stepper motor, continuous variable, and can input any speed within the range of the test protocol for shearing. Furthermore, the device has a relatively large shear box with a diameter of 185 mm (upper and lower shear box heights of 40 and 20 mm, respectively). The instrument loading device includes horizontal and vertical loading. The maximum horizontal load is up to 50 kN, and the maximum vertical load is 57.12

kg to generate a vertical stress of up to 400 kPa. The shear displacement and vertical deformation of the sample were measured using two displacement meters.

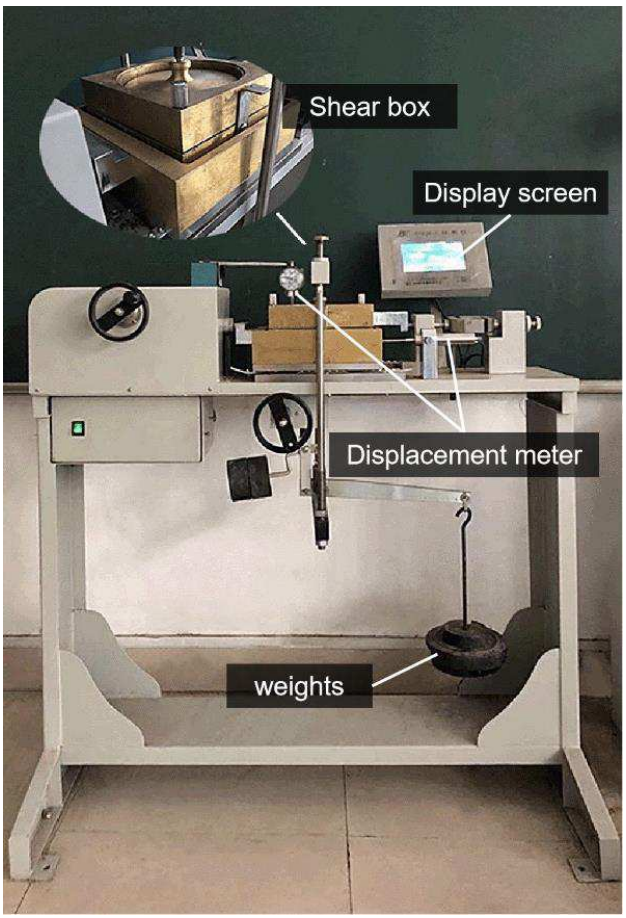

Figure 3 Direct shear test apparatus.

2.3 Text process

The horizontal displacement applied by the motor generates shear stress at a constant rate, and the shearing rate adjustment range is between 0.01 and 99.99

mm/min. Researchers (Fard et al. 2015, Zhan et al. 2015, Abreu et al. 2017) have conducted experiments on MSW or MBT waste and set a shearing displacement rate ranging from 0.2 to 19 mm/min; however, these studies did not consider the effect of shearing displacement rate on the material. Therefore, this study covers the above-mentioned rates and selects five shearing rates for comparison experiments: 0.25, 1, 5, 10, and 20 mm/min. The waste in the landfill is gradually piled up in layers during the landfill process, because of which, the landfill body will undergo compression and deformation accompanied by slipping instability allowing it to be simulated and studied. There were changes in the shear strength parameters of MBT waste with buried depth (10–100 m). The preparation of MBT waste samples included chopping it into particles <23 mm to ensure that the ratio of the maximum material particle size to the diameter of the shear box did not exceed 1:8 (CJJ/T 2013) (Figure 4). To ensure that the moisture content of each sample was consistent, the MBT waste sample with a moisture content of 20% was prepared before the DS test. The specific steps were as follows: a 700-g MBT waste sample was placed into an oven at 65 °C, the sample was dried for 24 ± 1 h, to a constant weight. Then, 140 g of purified water was used tosprayed evenly on the MBT waste soil with a watering can and the sample was turned the continuously. Finally, the sample was stewing for 24 ± 1 h.

Figure 4 MBT waste test materials.

The sample was placed in the shear box in 10 mm layers, and then, a simple tamping hammer was used to evenly compact the sample to ensure the same vertical settlement in the same plane to reach an initial unit weight of 4 kN/m^3. Table 3 lists all the samples and test parameters used in this study. A total of 50 samples were tested. The vertical stresses were 40, 80, 120, 160, 200, 240, 280, 320, 360, and 400 kPa. After compressing the sample for 1440 ± 60 min under continuous vertical pressure, the shearing test was performed. Finally, the specimens were sheared at constant and slow (0.25, 1, and 5 mm/min) or fast (10 and 20 mm/min) shearing rates. The horizontal load was recorded every time the specimen produced 1% shear horizontal displacement. The test ended when the ratio of the shear horizontal displacement to the sample diameter reached 20%.

205 Table 3 Specimen and test parameters.

Specimen number	Vertical pressure during compressing (σ, kPa)	Vertical pressure duration (min)	Total unit weight prior to shearing (γ, kN/m^3)	Shearing rate (mm/min)	Shear test duration (min)	Temperature (℃)
DS1-1	40	1440	5.12	0.25	149.1	28.5
DS1-2	80	1380	6.05	0.25	154.2	29.3
DS1-3	120	1380	6.31	0.25	154.1	28.7
DS1-4	160	1380	6.58	0.25	154.5	28.6
DS1-5	200	1350	6.81	0.25	154.1	28.9
DS1-6	240	1380	7.01	0.25	154.1	28.7
DS1-7	280	1380	7.25	0.25	154.1	28.9
DS1-8	320	1380	7.44	0.25	154.1	29.1
DS1-9	360	1380	7.62	0.25	154.5	29.3
DS1-10	400	1350	7.77	0.25	155.9	29.1
DS2-1	40	1440	5.12	1	37.2	26.2
DS2-2	80	1440	6.01	1	37.8	26.5
DS2-3	120	1440	6.32	1	37.1	26.6
DS2-4	160	1380	6.57	1	37.5	27.1
DS2-5	200	1560	6.81	1	38.5	26.5
DS2-6	240	1380	7.02	1	39.2	26.8
DS2-7	280	1440	7.22	1	38.6	26.5
DS2-8	320	1380	7.43	1	42.1	26.5
DS2-9	360	1380	7.62	1	37.8	27.1
DS2-10	400	1380	7.71	1	38.0	26.8
DS3-1	40	1380	5.15	5	8.1	28.6
DS3-2	80	1440	6..11	5	7.8	28.5
DS3-3	120	1400	6.38	5	7.9	28.7
DS3-4	160	1440	6.58	5	7.9	28.8
DS3-5	200	1380	6.90	5	7.7	29.1

DS3-6	240	1440	7.12	5	7.7	28.7
DS3-7	280	1440	7.25	5	7.7	28.7
DS3-8	320	1380	7.48	5	7.7	29.3
DS3-9	360	1380	7.67	5	7.8	28.9
DS3-10	400	1440	7.79	5	8.0	28.8
DS4-1	40	1380	5.11	10	3.9	26.9
DS4-2	80	1440	6.01	10	4.0	26.7
DS4-3	120	1400	6.32	10	4.0	27.6
DS4-4	160	1400	6.58	10	4.0	26.5
DS4-5	200	1440	6.80	10	4.0	27.1
DS4-6	240	1440	7.02	10	4.0	26.8
DS4-7	280	1400	7.23	10	4.0	26.9
DS4-8	320	1440	7.43	10	4.0	27.3
DS4-9	360	1440	7.62	10	3.9	27.1
DS4-10	400	1400	7.84	10	4.0	27.5
DS5-1	40	1440	5.21	20	2.0	27.5
DS5-2	80	1440	6.09	20	2.0	27.8
DS5-3	120	1440	6.35	20	2.0	27.5
DS5-4	160	1440	6.61	20	2.0	28.1
DS5-5	200	1380	6.90	20	2.0	28.3
DS5-6	240	1440	7.01	20	2.0	28.3
DS5-7	280	1440	7.25	20	2.0	28.1
DS5-8	320	1440	7.44	20	2.0	28.5
DS5-9	360	1380	7.63	20	2.0	28.7
DS5-10	400	1440	7.92	20	2.0	28.3

Note: DS - direct shear test.

3. Results and analysis

3.1 Consolidation phase

During the consolidation and compression stages, the specimen underwent

compression deformation. However, due to the low organic content and low moisture content of MBT waste, no drainage occurred during consolidation. The relationship between the porosity ratio of the sample and logarithm of the vertical pressure in the consolidation and compression stages is shows that as the vertical pressure increases, the void ratio gradually decreases (Figure 5); the relationship can be fitted into a straight line, the slope of the straight line (compression index) is 1.14, and the sample has high compressibility. Because the initial unit weight of the sample is 4 kN/m^3, when the vertical pressure increased from 40 to 400 kPa, it can simulate the self-weight stress of MBT waste from 10 m to 100 m. The weight of the MBT waste material is comparable to the simulated landfill depth; the relationship is shown in Figure 6. Figure 6 shows that as the self-weight stress increased, the unit weight of the material increased from 4.00 to 7.84 kN/m^3. The relationship between the porosity ratio of MBT waste materials and simulated landfill depth is shown in Figure 7. Figure 7 shows that the porosity ratio of MBT waste is generally larger than that of MSW, and the porosity ratio of deep MBT waste is close to that of shallow MSW waste.

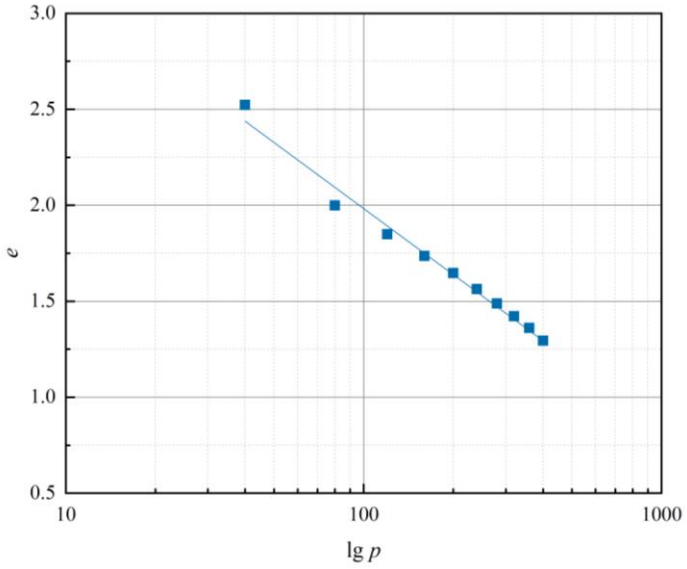

228

229 Figure 5 The relationship between the porosity ratio (e) and the logarithm of vertical pressure

230 (lg p).

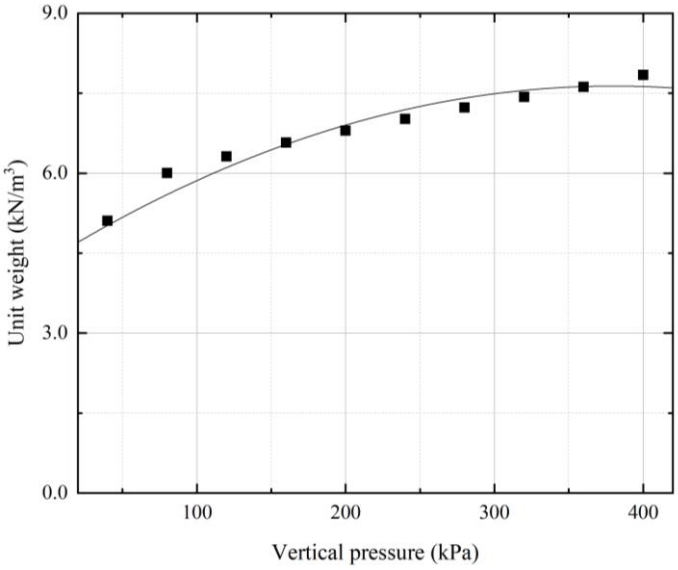

231

232 Figure 6 The relationship between the unit weight of the sample and the vertical pressure.

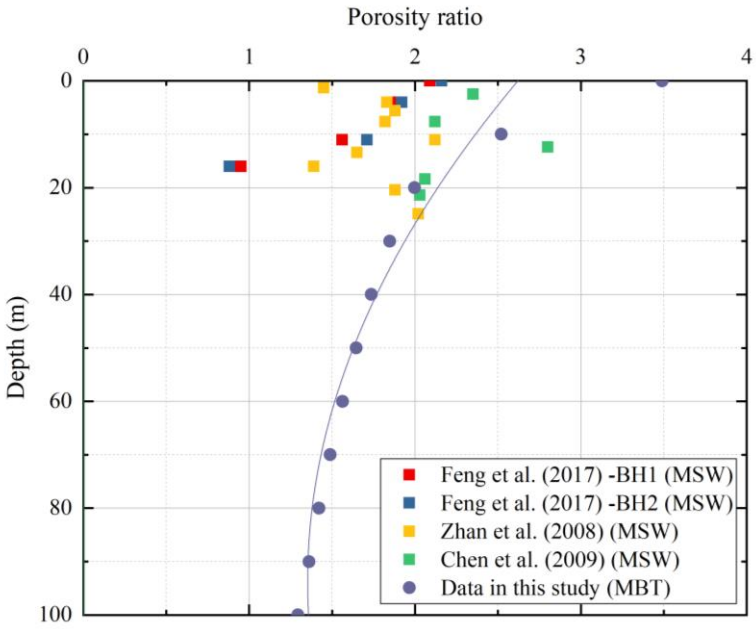

Figure 7 The porosity ratio of MSW and MBT waste varies with depth.

3.2 Shear stress-displacement behaviour

In this study, the DS stress–horizontal displacement graphs of all specimens show strain hardening, which is illustrated with a shearing rate of 5 mm/min (Figure 8). In all tests, the shear stress continued to increase until the horizontal displacement reached 37 mm (the ratio of horizontal displacement to sample diameter reached 20%). This is because the maximum displacement of the test equipment is 40 mm; therefore, the test must be interrupted when the horizontal displacement of the sample reaches 37.5 ± 0.5 mm. The value range of the horizontal displacement is the same as that performed by Zhan et al. (2008), Bray et al. (2009), Reddy et al. (2009a), Reddy

et al. (2009b), and Feng et al. (2017). The test settings are similar, and the maximum horizontal displacement values are all less than 35%. Therefore, even under relatively large displacements, displacement hardening is a common phenomenon in MBT waste.

The shear stress–horizontal displacement curve of the sample shows an upward convex trend. As the horizontal displacement increases, the shear stress increases rapidly. When the horizontal displacement of the specimen reached 9.25 mm (the ratio of horizontal displacement to sample diameter reached 5%), the growth rate of the shear stress changed from high speed to stable. The shear stress–horizontal displacement relationship of MBT waste is similar to that of general MSW (Zhang 2018c). The main reason for this phenomenon is that initially, the shear strength of the material is borne by the fine-grained aggregate, and as the horizontal displacement increases, it quickly rises to the ultimate shear strength of the aggregate. Subsequently, reinforced materials such as plastics are used as the main shear resistance components, and fibrous materials such as plastics will be stretched and deformed under the action of shear load. However, these materials are not easily broken by instantaneous breakage during the stretching process owing to their good toughness; however, like elastic materials, there is still a process of yielding before failure, showing reinforcement characteristics.

In this study, 10 different vertical pressures were applied to the sample to

simulate the landfill depth of MBT waste of 10–100 m. It can be clearly observed in Figure 8 that the shear strength obtained by the shear test of MBT waste increases with the increase in vertical pressure (landfill depth), which is different from the decrease in MSW shear strength with increasing depth (Cho et al., 2011; Feng et al., 2017). The main reason for this is that the composition of the material and physical properties of the material will change with an increase in the MSW landfill depth. Compared with deep MSW, shallow MSW has high degradability, high organic content, and relatively low water content; therefore, it has better shear performance in the shear test (Karimpour-Fard 2018). However, after MBT, as the depth of the landfill increases, the material content and moisture content do not change significantly; however, the void ratio decreases and the components are denser, which also increases the shear strength with the burial depth.

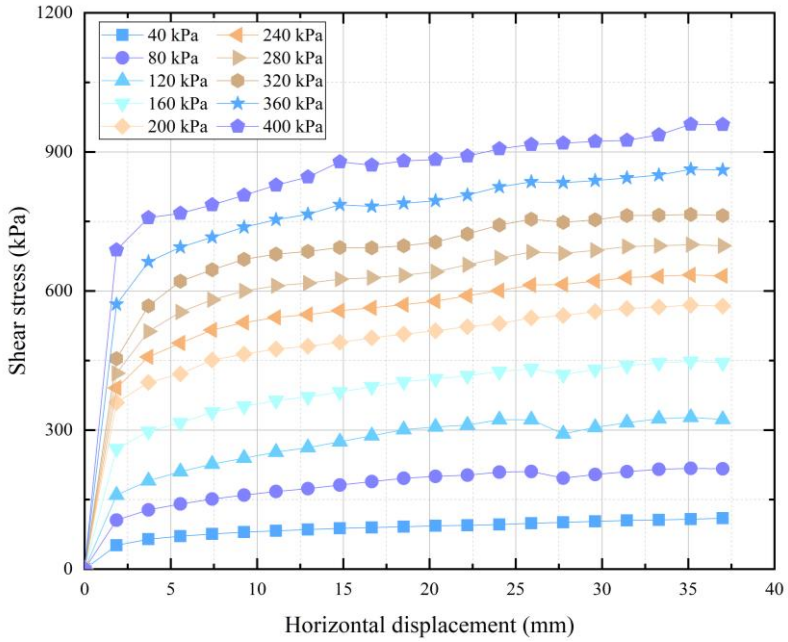

Figure 8 Shear stress-horizontal displacement graph (shearing rate is 5mm/min).

Since MBT waste does not have a distinct shear strength peak, the shear stresses when the shear strain reached 5, 10, 15, and 20% under each vertical pressure were taken as the shear strength under this pressure. Taking the 5 mm/min result as an example, the relationship between shear strength and vertical pressure is plotted (Figure 9). It can be seen from Figure 9 that with the increase in vertical pressure, the shear stress of the sample also increases, indicating that the larger the pressure, the denser the sample and larger the shear strength of the sample. Moreover, as the value of shear horizontal displacement increases, the shear strength of MBT waste increases; therefore, the value of horizontal displacement also affects the

290 determination of material shear strength.

291

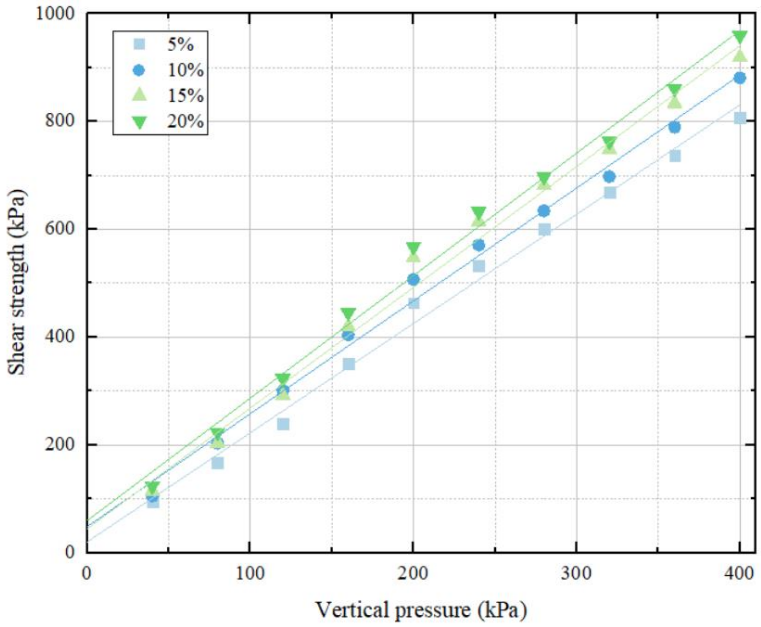

292

293 Figure 9 MBT waste shear strength envelope (shearing rate is 5mm/min).

294

295 ***3.3 Shear strength parameters in different shearing rate of MBT waste***

296 When the ratio of the shear horizontal displacement to the sample diameter under
297 each vertical pressure reaches 10 and 20%, the corresponding shear stress is taken as
298 the shear strength under the pressure. As can be seen in Figure 10, as the shearing rate
299 (logarithm) increases, the shear strength of the sample increases accordingly. This is
300 similar to applying a rapid impact load to MBT waste. It takes a certain amount of
301 energy to destroy MBT waste in a short time; therefore, the shear strength of MBT

302 waste was improved. Additionally, owing to the high ratio of plastic to textile in the
303 material, there were more large-sized strip-shaped plastics and textiles participating in
304 the force. In addition, in the case of larger shearing displacement rates (10 and 20
305 mm/min), it can be observed that the shear strength of the ratio of different shear
306 horizontal displacements to the sample diameter (10% and 20%) was not substantially
307 different. However, as the vertical pressure increased, the slope of the shear strength
308 line increased. This shows that choosing different shearing displacement rates and
309 shear displacements affects the shear strength. In addition, with a higher rate, although
310 the value of the shear displacement slightly effects the shear strength, different
311 vertical pressures have obvious changes in the shear strength of the material.
312

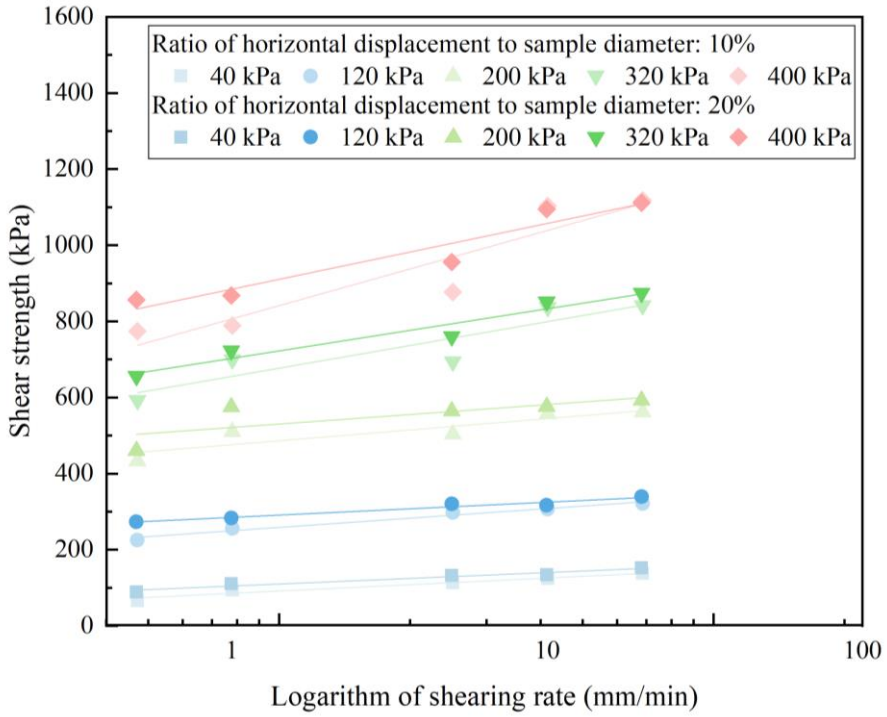

Figure 10 The relationship between shear strength and logarithm of shearing rate.

In order to better describe the correlation between shear strength and shearing rate, a shearing rate sensitivity coefficient β is introduced, formula (1).

$$\beta = \frac{S_i / S_0}{\log(V_i / V_o)} \tag{1}$$

where S_0 is the given initial shear stress (kPa), S_i is the shear stress (kPa) corresponding to the shearing rate, V_0 is the given initial shearing rate (mm/min), and V_i is the corresponding final shearing rate (mm/min).

Figure 11 shows that the shearing rate sensitivity coefficient can be fitted to a

323 straight line. The absolute value of the slope of the straight line is 1.61, and the
324 shearing rate sensitivity coefficient is between 0.64 and 2.66. The absolute value of
325 the slope of the line fitted by Zekkos et al. (2010) (test shearing rates are 0.1, 1, and 5,
326 respectively) is 0.71, and the rate sensitivity coefficient is between 0.5 and 1.0. The
327 absolute value of the slope of the line fitted by Karimpour-Fard et al. (2013) (test
328 shearing rates are 0.8, 8, and 19, respectively) is 0.55, and the shearing rate sensitivity
329 coefficient is between 0.8 and 1.2. As the increment between shearing rates increases,
330 the sensitivity between shear strength and shearing rate decreases. The linear slope of
331 the MBT waste sample in this test is greater than that of the MSW sample, and the
332 shear strength and shearing rate sensitivity of MBT waste are strong.
333

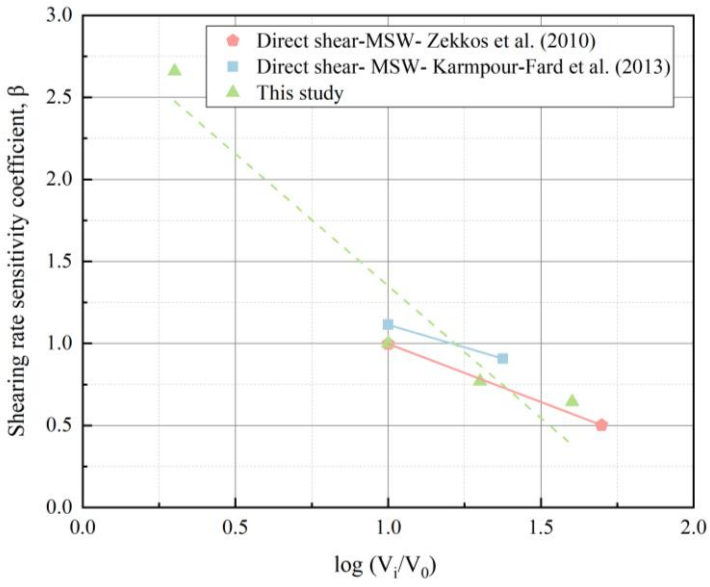

334

335 Figure 11 The shearing rate sensitivity coefficient of waste samples.

The shear strength parameters of MSW are calculated based on the Mohr–Coulomb theory. The shear strength parameters of the MBT waste were obtained. The relationship between the shear strength parameters c and φ of MBT waste with different shearing rates and ratio of shear displacement to sample diameter are shown in Figures 12 and 13. It can be seen from Figure 12 that the cohesion increases with the increase in the ratio of shear displacement to the sample diameter and with the increase in the shearing rate. When the ratio of shear displacement to sample diameter was 20%, the shearing rate increased from 0.25 to 20 mm/min, and the cohesive force increased from 22.32 to 39.51 kPa. In particular, in the slow shearing rate (0.25 mm/min) test at low ratio of shear displacement to sample diameter (5%), the shear strength of MBT waste is mainly caused by the friction angle, while the cohesion is negligible. Figure 13 shows that the internal friction angle increases with the increase of shearing rate, but has little relationship with the ratio of shear displacement to sample diameter. When the ratio of shear displacement to sample diameter was 20%, the shearing rate increased from 0.25 mm/min to 20 mm/min, and the internal friction angle increased from 64.24° to 68.52°, which is consistent with the results of Gao et al. (2010). The reason for the increase in cohesion and internal friction angle is that MBT waste becomes denser after consolidation and compression. The faster shearing rate makes the MBT waste material swell and produces negative pressure. Meanwhile,

band-shaped plastics and textiles are drawn to generate greater tensile stress, thereby increasing the shear strength parameters.

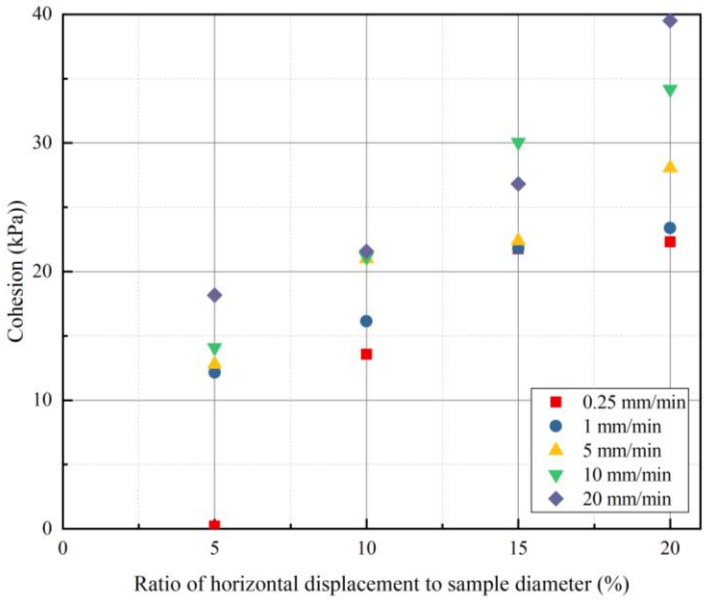

Figure 12 The relationship between cohesion and ratio of horizontal displacement to sample diameter.

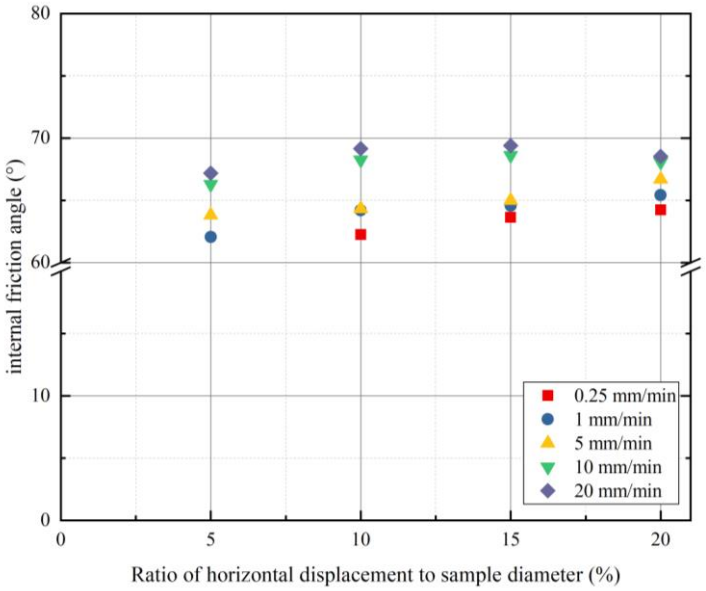

Figure 13 The relationship between internal friction angle and ratio of horizontal displacement to sample diameter.

3.4 Shear strength prediction theoretical model

The relationship among the shear strength, shearing rate, and vertical pressure of MBT waste is shown in Figure 14. Figure 14 shows that the shear strength of MBT waste increases with the increase in the shearing rate and vertical pressure. The relationship between the shear strength of MBT waste and the shearing rate and vertical pressure can be fitted to a non-linear surface. The fitting equation is shown in equation (2), and the fitting correlation coefficient R^2 is 0.98, which shows a high degree of fit.

$$\tau_f = Z_0 + Bp + Cv + Dp^2 + Ev^2 \quad (2)$$

where τ_f is the shear strength of the material (kPa), p is the normal stress (kPa), v is the shearing rate (mm/min), and the fitting coefficients Z_0, B, C, D, and E are the fitting correlation coefficients (Table 4).

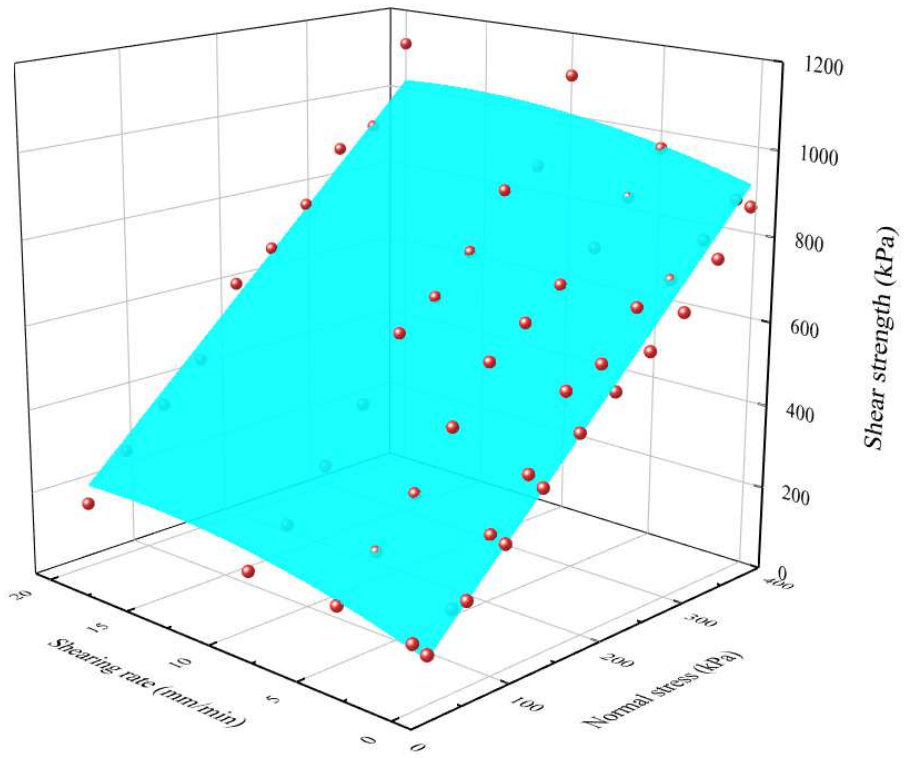

Figure 14 Shear strength fitting model.

384 Table 4 Fitted correlation coefficient.

Z_0	-3.56 ± 0
B	2.26 ± 0.03
C	13.75 ± 0.69
D	4.82E-5 ± 0
E	-0.41 ± 0
R^2	0.98

385

386 As shown in Figure 15, the relationship between the cohesion and the logarithm
387 of the shearing rate can be fitted to a straight line, and the average value of the fitting
388 correlation coefficient R^2 is 0.91. The degree of fit is relatively high, and the fitted
389 straight-line equation is shown in equation (3). As can be seen in Figure 16, the
390 relationship between the internal friction angle and the logarithm of the shearing rate
391 can be fitted to a straight line, and the average value of the fitting correlation
392 coefficient R^2 is 0.91. The degree of fit is relatively high, and the fitted straight-line
393 equation is shown in equation (4).

394
$$\begin{cases} c = 8.790 logv + 25.274 & (\varepsilon = 10\%) \\ c = 4.562 logv + 16.495 & (\varepsilon = 20\%) \end{cases} \quad (3)$$

395
$$\begin{cases} \varphi = 2.294 logv + 65.492 & (\varepsilon = 10\%) \\ \varphi = 3.478 logv + 63.962 & (\varepsilon = 20\%) \end{cases} \quad (4)$$

396 where c is the cohesive force (kPa) of the material, v is the shearing rate
397 (mm/min), ε is the ratio of the horizontal displacement to the sample diameter, and φ

is the internal friction angle of the material (°).

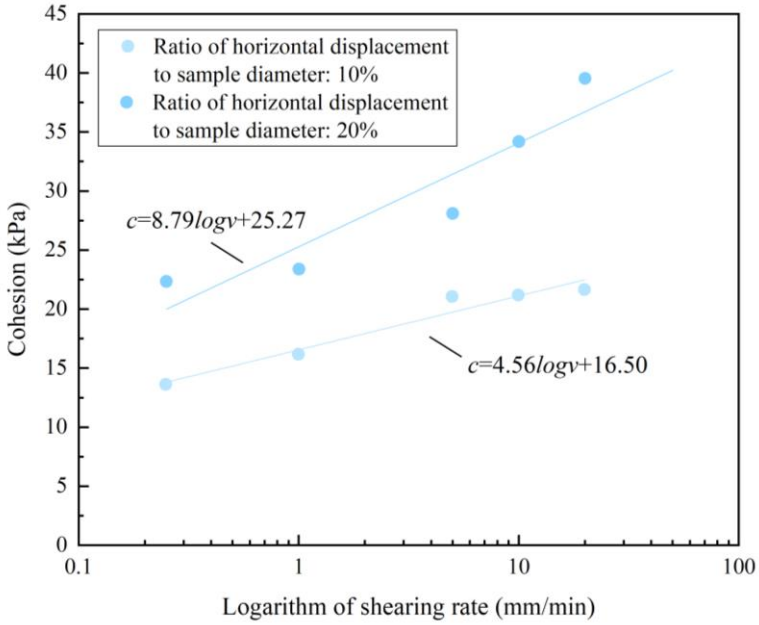

Figure 15 Relationship between cohesion and logarithm of shearing rate.

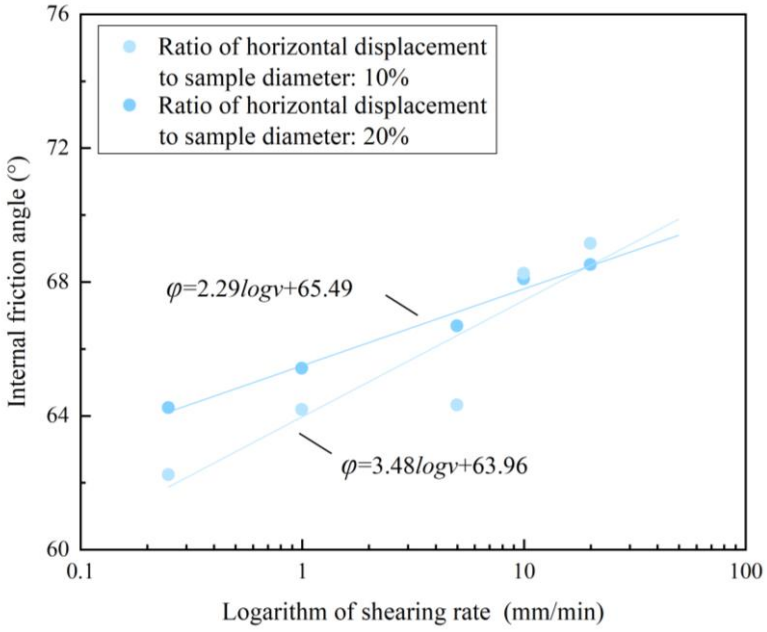

Figure 16 Relationship between internal friction angle and logarithm of shearing rate.

4. Discussion

4.1 Sample moisture content

We selected 18 references to compare the moisture content of HT landfill MBT waste (Figure 17). It can be seen from Figure 17 that the moisture content is generally distributed between 20-60%, among which the moisture content of MBT waste is between 18-40%, and the moisture content of MSW is between 20-100%. The moisture content of MBT waste is generally lower than that of MSW, and the range of variation is small. The main reason is that MBT technology removes most of the organic matter in MSW and greatly reduces the moisture content of the material

through air drying.

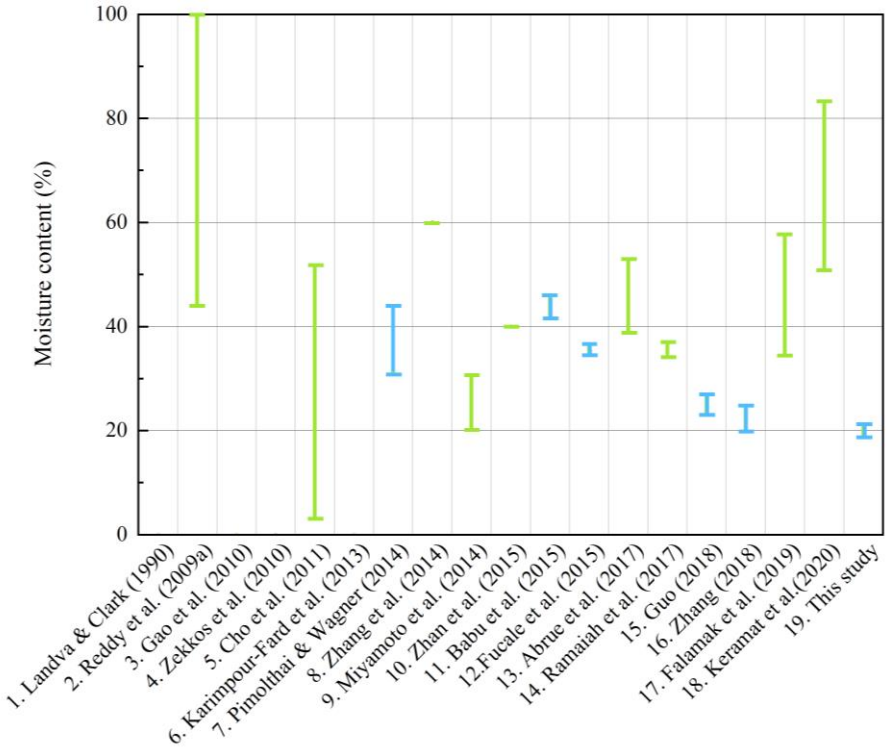

Figure 17 Moisture content of each reference sample (green - MSW, blue - MBT waste).

4.2 Sample unit weight

The unit weight of the sample is shown in Figure 18. The unit weights of MBT waste, MSW, and HT-MBT waste are between 5.3-12.4 kN/m^3, 3.5-14.1 kN/m^3, and 4-8 kN/m^3, respectively. Between them, The HT-MBT waste is generally smaller than the heavy range of other MSW and MBT waste. By comparing the composition of these wastes, it is observed that the percentage of plastic content in the MBT waste

materials in HT landfill is higher than that of the above materials. On the one hand, considering that most of the organic materials are eliminated, the unit weight of MBT waste is lower. On the other hand, due to poor recycling awareness and different consumption patterns, the increase in the percentage of low-weight and large-volume plastics may also be the reason why the unit weight of MBT waste is relatively low.

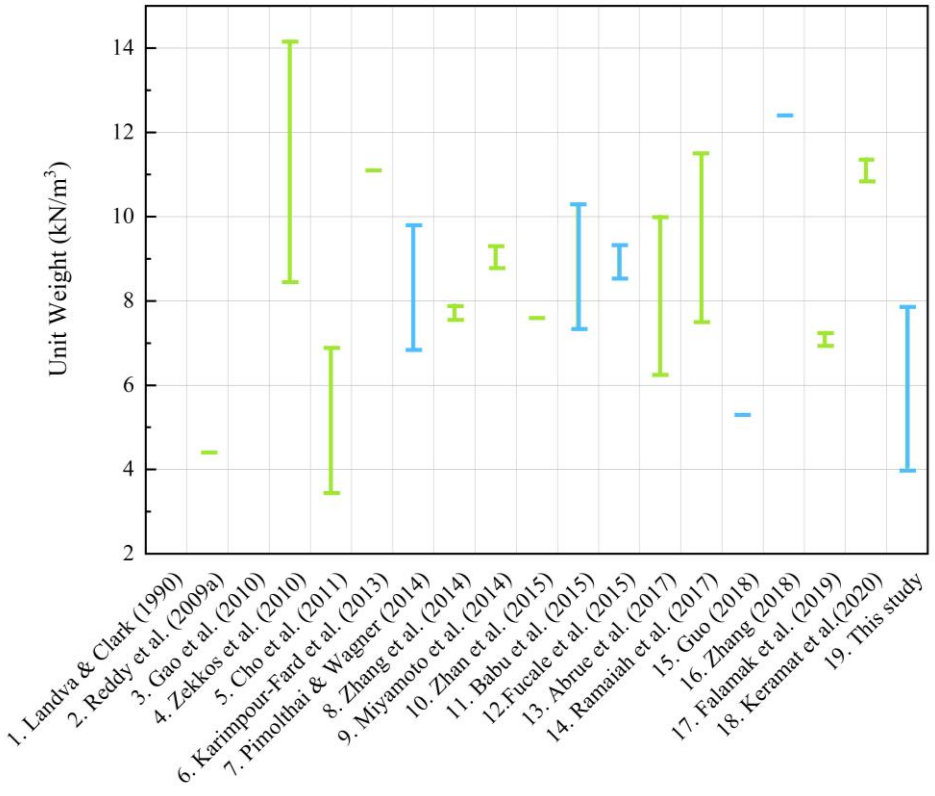

Figure 18 Unit weight of each reference sample (green - MSW, blue - MBT waste).

4.3 Test parameters

Table 5 lists the experimental parameters used in the references. Many scholars have provided results of on-site (Miyamoto et al. 2014, Keramat et al. 2020), or laboratory direct shearing of MSW or MBT waste. The largest sample size for laboratory research reaches 860 × 860 × 620 mm, the smallest is 60 × 60 × 30 mm, and the size of in site test samples can reach 1220 × 1220 × 750 mm. Further, the DS test device is divided into square and round shapes; the test shear box used in this study was a relatively large round shear box. The range of vertical pressure applied was 2–774 kPa, and the vertical pressure range for most of the tests was 50–200 kPa. The duration of the pressure application is generally ~1440 min. Most of the literature research content includes material composition, moisture content, buried depth, severity, age, fibre orientation, void ratio, particle size, top overburden pressure, upper earth pressure, and self-weight stress on MSW/MBT shear impact of intensity. Only Zekkos et al. (2010) and Karimpour-Fard et al. (2013) studied the effect of multiple shearing rates on shear strength. Zekkos et al. (2010) studied the effects of different components, unit weights, and shearing rates on the shear strength of MSW. The shearing rates were 0.1, 1, and 5 mm/min, and the vertical pressures were 2, 50, and 150, 370, and 700 kPa and held for 1440 min. The test results show that the greater the depth in the landfill, the greater the reduction of the internal friction angle, and that the shear strength is likely to correspond to the weakest direction of the shear

plane. Karimpour-Fard et al. (2013) studied the influence of fibre content, fibre orientation, age, and shearing rate on MSW, applying 20, 50, 100, and 200 kPa vertical pressures and maintaining them for 1440 min. The shearing rate was set to 0.8, 8, and 19 mm/min. The results show that as the shearing rate increased, as did the shear strength of MSW. When the horizontal displacement was 1.5, 3, and 4.5 cm, the shear strength of MSW increased to 27%, 22%, and 16%, respectively. The sensitivity coefficient is up to 0.33. This study investigates the effect of shearing rate on the strength of MBT waste materials, and the set rate covers the above-mentioned rates. A vertical pressure of 40–400 kPa was applied to simulate the self-weight stress at a landfill depth of 10–100 m.

Table 5 Reference test parameters.

Number	Reference	Sample type	Vertical stress duration (min)	Testing method and sample size (mm)	Displacement or strain at the shearing resistance considered and vertical pressure (kPa)
1	Landva & Clark (1990)	MSW	NA	L-DS, 434×287	PS, 30.3-565
2	Reedy et al. (2009)	MSW	NA	L-DS, 70(D)	PD(15%), 176-774
3	Gao et al. (2010)	MSW	120	L-DS, 300×300×150	PD(6.7% and 10%), 50-300
4	Zekkos et al. (2010)	MSW	1440	L-DS, 300×300×180	PD(55mm), 2-700
5	Cho et al. (2011)	MSW	240-1800	L-DS, 100(D) 860×860×620	PD(18%), 48-290 PD(30%), 96-287
6	Karimpour-Fard et al. (2013)	MSW	1440	L-DS, 300×300×150	PD(5, 10 and 15%), 20-200

7	Pimolthai & Wagner (2014)	MBT-MSW	NA	L-DS, 94(D)	PS, 20-100
8	Zhang et al. (2014)	MSW	0-1440	L-DS, 150(D)	PD(20%), 25-200
9	Miyamoto et al. (2014)	MSW	10	I-DS, 300×150	PD(40mm), 8.2-13.6
10	Zhan et al. (2015)	MSW	30-740	L-DS, 618(D)	PD(10%), 12.5-100
11	Babu et al. (2015)	MBT-MSW	NA	L-DS, 60×60×30	PD(20%), 50-150
12	Fucale et al. (2015)	MBT-MSW	4320	L-DS, 100×100×150	PD (20%), 100-300
13	Abrue et al. (2017)	MSW	250	L-DS,500×500×500	PD(20%), 50-250
14	Ramaiah et al. (2017)	MSW	700	L-DS, 305×305×203	PD(55mm), 25-200
15	Guo (2018)	MBT-MSW	1440	L-DS, 180(D)	PD(10%, 15%), 50-200
16	Zhang (2018)	MBT-MSW	1440	L-DS, 200(D)	PD(20%), 12.5-200
17	Falamak et al. (2019)	MSW	1440	L-DS, 300×300×165	PS, 50-200
18	Keramat et al. (2020)	MSW	NA	I-DS, 1220×1220×750	PD(4%), 6.7-22.2
19	This study	MBT-MSW	1440	L-DS, 185(D)	PD(5%, 10%, 15% and 20%), 40-400

L laboratory tests, I in-site tests, DS direct shear, PS peak stress, PD peak displacement, NA not available.

4.4 Shear strength parameters

We collected references with a time span of up to 30 y (1990-2020), extracted shear strength parameters (data with similar strain values) obtained at various shearing rates in the literature. The influence of shearing rate on the shear strength parameters of materials was compared (Figure 19).

Figure 19 shows that as the shearing rate increases, the shear strength parameters c and φ of MSW and MBT waste also increase. The variation range of MSW cohesion is generally between 0–46 kPa, and cohesion range of MBT waste is concentrated

between 5.4–39.5 kPa (some data points with larger increases are excluded), and the range of MSW cohesion larger than MBT waste. The MSW internal friction angle range was 7–50.6°, and the MBT waste internal friction angle range was 17.2–48.1°; most fluctuate around 30°. The internal friction angle range of this study was 59.92–68.52°, which is generally greater than the conclusions of other literature. The main reasons for the difference in shear strength parameters of MSW and MBT waste are the different components of the materials and different shearing rates. Different components and different shearing rates will show different physical and mechanical properties. In addition, MBT pre-treatment technology has only been studied by scholars in some countries, which also partly explains the small range of test results.

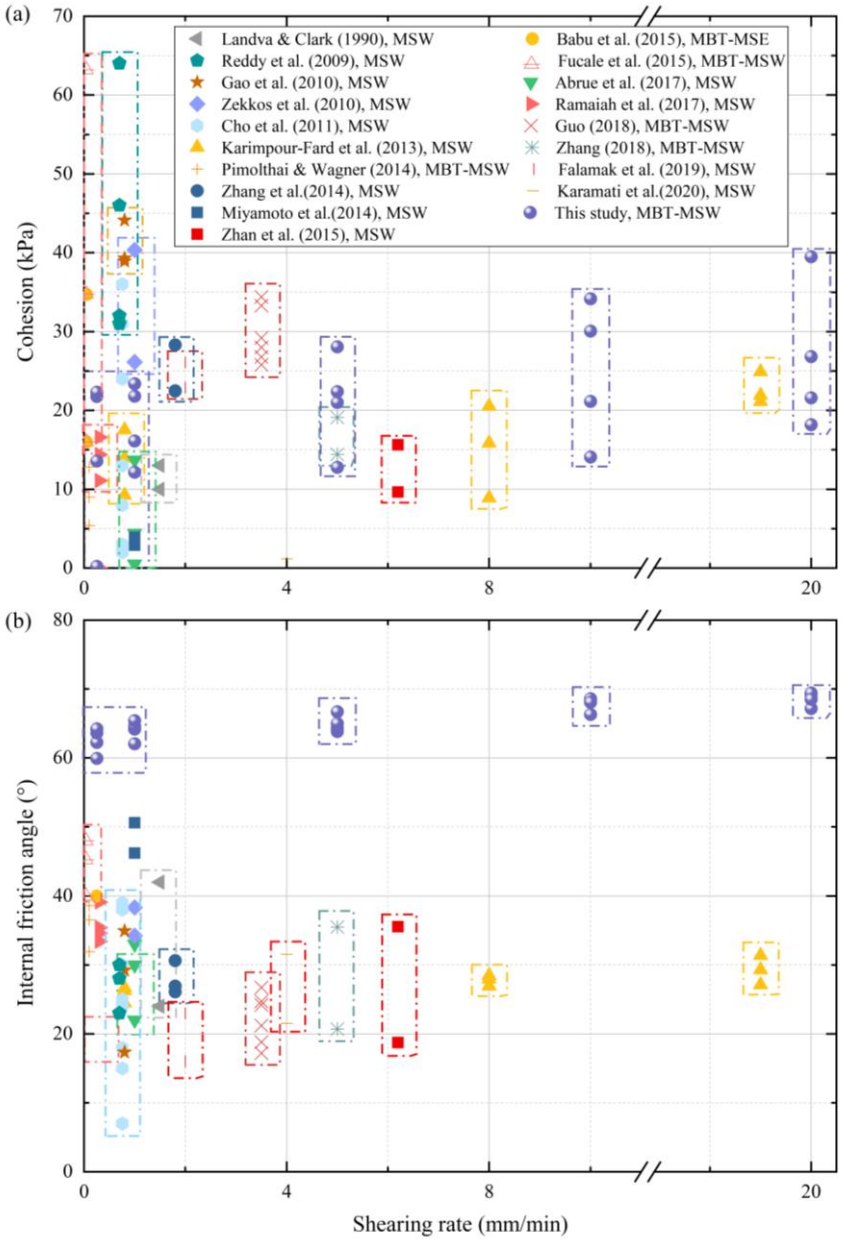

Figure 19 Comparison of shear strength parameters (a) the relationship between cohesion and shearing rate, (b) the relationship between internal friction angle and shearing rate.

5. Conclusion

To supplement the relationship between MBT waste in shearing rate, landfill depth and shear strength. In this study, the direct shear test was used to test the MBT waste, and the experimental phenomenon that the shear strength increases with shearing rate increases. Furthermore, a theoretical model of shear strength prediction was established, and the range of shear strength parameters was obtained. The findings of this work provide basic data and strength models for the design, instability and damage prediction of MBT landfills. The specific conclusions are as follows:

(1) MBT waste was mainly composed of paper, plastic, rubber, textile, wood, stone, ceramics, glass, metal, fine-grained soil, and other visually indistinguishable materials. Among them, plastic and rubber are the most important in MBT waste ingredients (23.3% dry mass). The measured moisture content was 20%, which is significantly lower than that of MSW. The measured specific gravity was 1.53.

(2) With an increase in the horizontal displacement of MBT waste, the shear stress of the sample does not exhibit an obvious peak, indicating a displacement hardening phenomenon. MBT waste complies with the Mohr–Coulomb theory. As the value of shear horizontal displacement increases, the shear strength of MBT waste increases.

(3) A DS test instrument was used to study the influence of different shearing rates on the shear strength of MBT waste. The test results show that as the shearing

513 rate increased, the shear strength of MBT waste increased. The sensitivity coefficient
514 between the shearing rate and shear strength of MBT waste was 0.64-2.66.
515 (4) A DS test instrument was used to simulate the influence of different landfill
516 depths on the shear strength of MBT waste. The test results show that the shear
517 strength increased with an increase in the buried depth.
518 (5) We established an MBT waste shear strength prediction model considering
519 the effects of shearing rate and normal stress simultaneously. This model can simulate
520 and predict the changes in MBT waste shear strength with shearing rate and vertical
521 pressure. The model was fitted into a nonlinear smooth surface in a rectangular
522 coordinate system with a fitting coefficient of 0.98.
523 (6) The relationship between cohesion c and the logarithm of the shearing rate
524 can be fitted to a straight line, with an average fitting coefficient of 0.91. The law
525 conforms to the logarithmic model, and the expression of the logarithmic model is
526 established. The cohesive force increased with the increase in the shearing rate and
527 with the increase in horizontal displacement.
528 (7) The relationship between the internal friction angle φ and logarithm of the
529 shearing rate, log$v$, could be fitted to a straight line, with an average fitting coefficient
530 of 0.91. The law conformed to the logarithmic model, and the expression of the
531 logarithmic model was established. In contrast to the cohesive force, the slope of the
532 straight line with ε = 20% was less than ε = 10%. This is because under large

horizontal shear displacement, some of the reinforced materials are broken and damaged, and the effect of the reinforcement is weakened.

(8) The cohesion c of MBT waste was in the range of 22.32–39.51 kPa, and the internal friction angle φ was in the range of 64.24°-68.52°.

Ethics approval and consent to participate

Not applicable.

Consent for publication

Not applicable.

Availability of data and materials

The datasets used and/or analysed during the current study are available from the corresponding author on reasonable request.

Competing interests

The authors declare that they have no competing interests.

Funding

This research was funded by the National Natural Science Foundation of China (Contract Nos. 51978625 and 51678532) and supported by Zhejiang Provincial Natural Science Foundation of China under Grant No. LZ21E080003.

Authors' contribution

552 Jiahe Zhang conducted the direct shear test on Hangzhou Tianziling MBT waste,
553 and analyzed and interpreted the influence of shearing rate on the shear strength of
554 MBT waste. Qiaona Wang, Min Wang and Chenyu Nie conducted the direct shear test
555 on Hangzhou Tianziling MBT waste, Zhenyiing Zhang analyzed the test data, and
556 reviews and revises the full text. All authors read and approved the final manuscript.
557
558 **Acknowledgements**
559 Thanks for the help of the Hangzhou Environmental Group.
560
561 **References**
562 Abreu AES and Vilar OM (2017) Influence of composition and degradation on
563 the shear strength of municipal solid waste. *Waste Management* 68: 263-274.
564 Archer E, Baddeley A, Klein A, Schwager J, Whiting, K (2005) Mechanical-
565 Biological Treatment: A guide for decision makers processes, policies, markets.
566 Juniper Consultancy Services Ltd, Uley, England., pp. 650.
567 Babu GLS, Lakshmikanthan P, Santhosh LG (2015) Shear strength characteristics
568 of mechanically biologically treated municipal solid waste (MBT-MSW) from
569 Bangalore. *Waste Management* 39(5): 63-70.
570 Bareither CA, Benson CH, Edil TB (2012) Effects of Waste Composition and
571 Decomposition on the Shear Strength of Municipal Solid Waste. *Journal of*

572 *Geotechnical and Geoenvironmental Engineering* 138(10): 1161-1174.

573 Bhandari AR and Powrie W (2013) Behavior of an MBT waste in monotonic
574 triaxial shear tests. *Waste Management* 33: 881-891.

575 Bray JD, Zekkos D, Kavazanjian E, Athanasopoulos GA, Riemer MF (2009)
576 Shear strength of municipal solid waste. In: International Symposium on Waste
577 Mechanics 1356: 709–722.

578 Cho YM, Ko JH, Chi L, Townsend TG (2011) Food waste impact on municipal
579 solid waste angle of internal friction. *Waste Management* 31: 26-32.

580 Eskandari M, Homaee M, Falamaki A (2016) Landfill site selection for municipal
581 solid wastes in mountainous areas with landslide susceptibility. *Environmental*
582 *Science and Pollution Research* 23(12):12423–12434.

583 Falamaki A, Ghareh S, Homaee M, Hamtaeipour Shirazifard A, Abedpour S,
584 Kiani S, Mousavi N, Rezaei M, Motlagh MT, Nouri A (2019) Laboratory Shear
585 Strength Measurements of Municipal Solid Waste at Room and Simulated In Situ
586 Landfill Temperature, Barmshoor Landfill, Iran. *International Journal of*
587 *Environmental Science and Technology* 18: 185-197.

588 Falamaki A, Ghareh S, Homaee M, Shirazifard AH, Abedpour S, Kiani S, et al.
589 (2019) laboratory shear strength measurements of municipal solid waste at room and
590 simulated in situ landfill temperature, Barmshoor landfill, Iran. *International Journal*
591 *of Civil Engineering* 18: 185-197.

592 Fard MK, Shariatmadari N, Keramati M, Kalarijani HJ (2015) An experimental
593 investigation on the mechanical behavior of MSW. *International Journal of Civil*
594 *Engineering* 12(4): 292-303.
595 Fei XH and Zekkos D (2017) Comparison of direct shear and simple shear
596 responses of municipal solid waste in USA. *Journal of Environmental Geotechnics*
597 5(3): 158-167.
598 Feng SJ, Gao KW, Chen YX, Li Y, Zhang LM, Chen HX (2017) Geotechnical
599 properties of municipal solid waste at Laogang Landfill, China. *Waste Management*
600 63: 354-365.
601 Fernando VI and Sudarshana CK (2011) Shear strength characteristics of
602 mechanically biologically treated (MBT) waste. *University of Southampton.*
603 Frenando S, Powrie W, Wastson G, Richards DJ (2009) The Impact of the
604 reinforce content on the shear strength of mechanically biologically treated waste. In:
605 Third International Workshop “Hydro-Physico-Mechanics of Landfills” 3: 10-13.
606 Fucale S, Juca JFT, Muennich K (2015) The mechanical behavior of MBT waste.
607 *Electronic Journal of Geotechnical Engineering* 20(13): 5927–5931.
608 Fucale SP (2005) Influência dps componentes de reforço na resistência de
609 resíduos sólidos urbanos. *Federal University of Pernambuco, Brazil*, 219 p.
610 Gao W, Chen Y, Zhan L, Bian X (2015) Engineering properties for high kitchen
611 waste content municipal solid waste. *Journal of Rock Mechanics & Geotechnical*

612 *Engineering* (6):646-658.

613 Gao W, Tu F, Xiao C, Ke Q, Xie Z (2010) Experimental study on repeated direct
614 shear of municipal solid waste from different depth of landfill. *Chinese Journal of*
615 *Environmental Engineering* 4(5): 1171-1176.

616 Guerrero LA, Maas G, Hogland W (2013) Solid waste management challenges for
617 cities in developing countries. *Waste Management* 33(1):220–232.

618 Guo WQ (2018) Laboratory study on the strength characteristics of MBT waste.
619 *Zhejiang Sci-tech University* (in Chinese).

620 Jones DRV & Dixon N (2015) Landfill lining stability and integrity: the role of
621 waste settlement. *Geotextiles & Geomembranes* 23(1): 27–53.

622 Jones DRV, Taylor DP, Dixon N (1997) Shear strength of waste and its use in
623 landfill stability. In: Yong, R.N., Thomas, H.R. (Eds.), Proceedings Geoenvironmental
624 Engineering Conference. Thomas Telford, pp. 343–350.

625 Karimpour-Fard M (2018) Rehabilitation of Saravan dumpsite in Rasht, Iran:
626 geotechnical characterization of municipal solid waste. *International Journal of*
627 *Environmental Science & Technology* 16: 4419-4436.

628 Karimpour-Fard M (2018) Rehabilitation of Saravan dumpsite in Rasht, Iran:
629 geotechnical characterization of municipal solid waste. *International Journal of*
630 *Environmental Science & Technology* 16(8): 4419-4436.

631 Karimpour-Fard M, Machado SL, Shariatmadari N, Noorzad A (2010) A

632 laboratory study on the MSW mechanical behavior in triaxial apparatus. *Waste*
633 *Management* 8(31): 1807-1819.

634 Karimpour-Fard M, Shariatmadari N, Keramati M, Jafari-Kalarijani H (2013) An
635 experimental investigation on the mechanical behavior of MSW. *International*
636 *Journal of Civil Engineering* 12(4):292-303.

637 Kavazanjian N, Matascovic R, Bonaparte GR, Schmertmazin E (1995) Evaluation
638 of evaluation of MSW properties for seismic analysis. Geoenviron. 2000, Geotech.
639 Special Publ. ASCE. 46, 1126–1141.

640 Keramati M, Shahedifar M, Aminfar MH, Alagipuor H (2020) Evaluation the
641 Shear Strength Behavior of aged MSW using Large Scale In Situ Direct Shear Test, a
642 case of Tabriz Landfill. *International Journal of Civil Engineering* 18: 717-733.

643 Kuehle-Weidemeier M (2004) Landfilling of mechanically-biologically pretreated
644 municipal solid waste. *International Symposium Waste Management, Zagreb*, VIII.

645 Landva AO and Clark JI (1990) Geotechnics of waste fill. Geotechnics of waste
646 fills-theory and practice, ASTM STP 1070. In: Landva, A., Knowles, D. (Eds.),
647 American Society for Testing and Materials. Philadelphia, Pennsylvania, pp 86–103.

648 Machado SL, Carvalho FM, Vilar OM (2002) Constitutive model for municipal
649 solid waste. *Journal of Geotechnical and Geoenvironmental Engineering*, 128 (11):
650 940–951.

651 Mahler CF and Neto ADL (2006) Effect of fibre on shear strength of residue from

652 mechanical biological pretreatment of waste. *International Journal of Environment &*
653 *Waste Management* 1(1): 85-93.

654 Manassero M, Van Impe WF, Bouazza A (1996) Waste disposal and containment.
655 Proc. 2nd Int. Cong. Environ. Geotech. Osaka, Japan 3, 1425–1474.

656 Miyamoto S, Yasufuku N, Ishikura R, Omine K, Yamawaki A (2014) In-situ
657 shearing response and shear strength of various solid waste ground focused on fibrous
658 materials composition. In: TC105 ISSMGE International Symposium on
659 Geomechanics from Micro to Macro, 1357-1362.

660 Petrović I and Bauer E (2011) A simple hypoplastic model for simulating the
661 mechanical behaviour of MBT waste. Computational Geomechanics, COMGEO II-In
662 Proceedings of the 2nd International Symposium on Computational Geomechanics
663 pp: 337–346.

664 Pimolthai P and Wagner JF (2014) Soil mechanical properties of MBT waste
665 from Luxembourg, Germany and Thailand. *Songklanakarin Journal of Science and*
666 *Technology* 36(6):701-709.

667 Ramaiah BJ, Ramana GV, Datta M (2017) Mechanical characterization of
668 municipal solid waste from two waste dumps at Delhi, India. *Waste Management* 68:
669 275-291.

670 Reddy KR, Gangathulasi J, Parakalla NS, HettiarachchiH, Bogner JE, Lagier T
671 (2009b) Compressibility and shear strength of municipal solid waste under short-term

672 leachate recirculation operations. *Waste Management* 27(6): 578-587.

673 Reddy KR, Hettiarachchi H, Parakalla NS, Gangathulasi J, Bogner JE (2009a)
674 Geotechnical properties of fresh municipal solid waste at Orchard Hills Landfill,
675 USA. *Waste Management* 29(2):952-959.

676 Singh S, Murphy B (1990) Evaluation of the stability of sanitary landfills.
677 Geotech. Waste Fills – Theory Pract. ASTM STP 1070: 240–258.

678 Stark, T.D., Sarihan, N.H., Li, G (2009) Shear strength of municipal solid waste
679 for stability analyses. *Environmental Geology* 57, 1911–1923.

680 Tatsuoka F, Di Benedetto H, Enomoto T, Kawabe S, Kongkitkul W (2008)
681 Various viscosity types of geomaterials in shear and their mathematical expression,
682 *Soil and Foundation* 1(48): 41-60.

683 Zekkos D and Fei XH (2016) Constant load and constant volume response of
684 municipal solid waste in simple shear. *Waste Management* 63(5): 380-392.

685 Zekkos D, Athanasopoulos GA, Bray JD, Grizi A, Theodoratos A (2010) Large-
686 scale direct shear testing of municipal solid waste. *Waste Management* 30: 1544-1555.

687 Zekkos DP (2005) Evaluation of static and dynamic properties of municipal solid
688 waste. A dissertation submitted in partial satisfaction of the requirements for the
689 degree of Doctor of Philosophy in Geotechnical Engineering, *University of*
690 *California, Berekeley*.

691 Zhan TLT, Chen YM, Ling WA (2008) Shear strength characterization of

692 municipal solid waste at the Suzhou landfill, China. *Engineering Geology* 97(3-4): 97-
693 111.

694 Zhan XD, Yan LJ, Wu DZ, Zhang ZY (2015) Ultra-large direct shear test for
695 shear strength properties of artificial municipal solid waste. *Journal of Engineering*
696 *Geology* 23(5): 930-936.

697 Zhang Y (2018c) Research on municipal solid waste output forecast and MBT
698 volume reduction technology. *Zhejiang Sci-tech University* (in Chinese).

699 Zhang ZY, Yan LJ, Wu DZ (2014) Experimental study of compression and direct
700 shear combined test. *Rock and Soil Mechanics* 35(11): 3049-3055.

701 Zhang ZY, Yan LJ, Wu DZ, Zhang LF , Fu J, Hu YJ (2015) Experimental study
702 on shear strength parameters of fresh municipal solid waste. *Chinese Journal of*
703 *Geotechnical Engineering* 37(3): 432-439.

704 Zhang ZY, Zhang YX, Wang YF, Xu H, Guo WQ, Wu DZ, Fang YH (2018a)
705 Physical and Mechanical Characteristics of MBT Waste in China. In: Farid A., Chen
706 H. (eds) Proceedings of GeoShanghai 2018 International Conference:
707 Geoenvironment and Geohazard. GSIC 2018. Springer, Singapore.
708 https://doi.org/10.1007/978-981-13-0128-5_46.

Figures

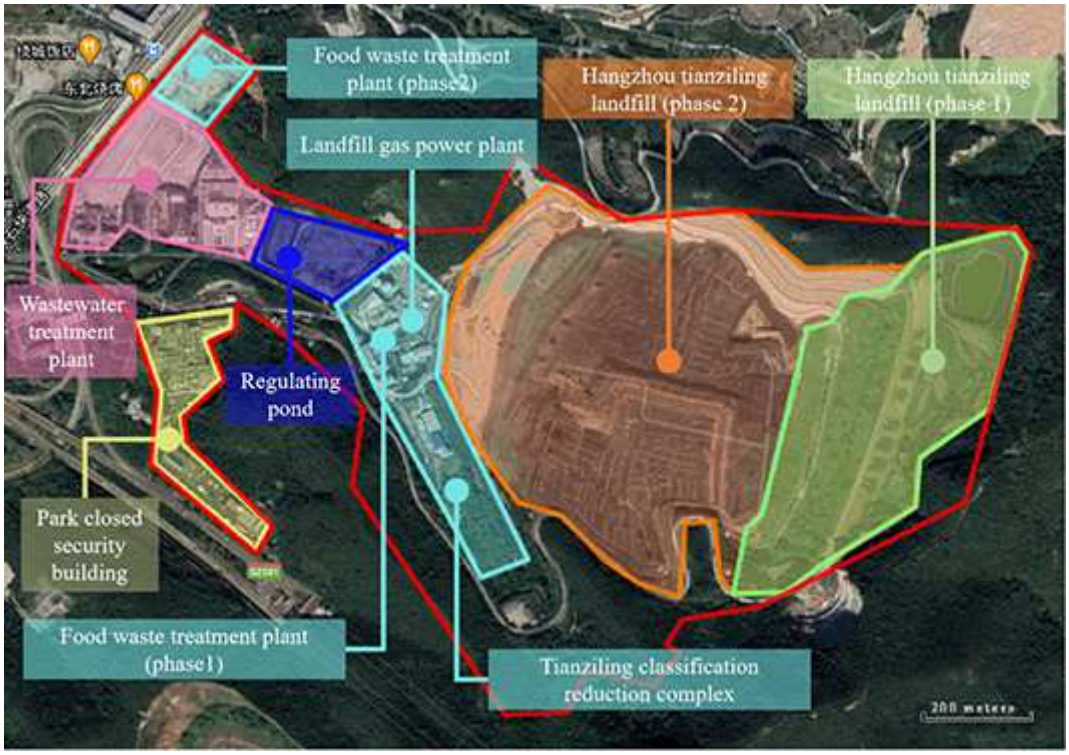

Figure 1

Floor plan of Hangzhou Tianziling Landfill, China. Note: The designations employed and the presentation of the material on this map do not imply the expression of any opinion whatsoever on the part of Research Square concerning the legal status of any country, territory, city or area or of its authorities, or concerning the delimitation of its frontiers or boundaries. This map has been provided by the authors.

Figure 2

MBT waste original materials.

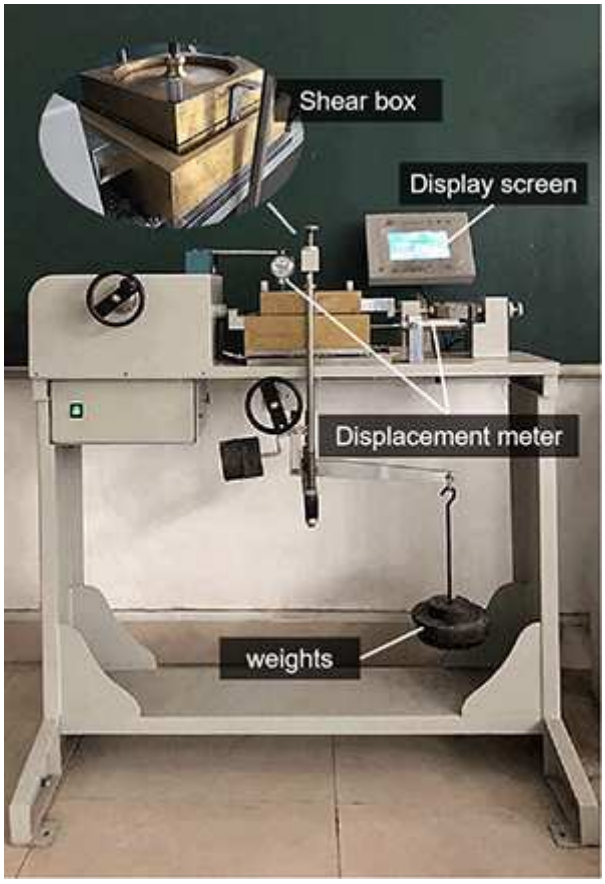

Figure 3

Direct shear test apparatus.

Figure 4

MBT waste test materials.

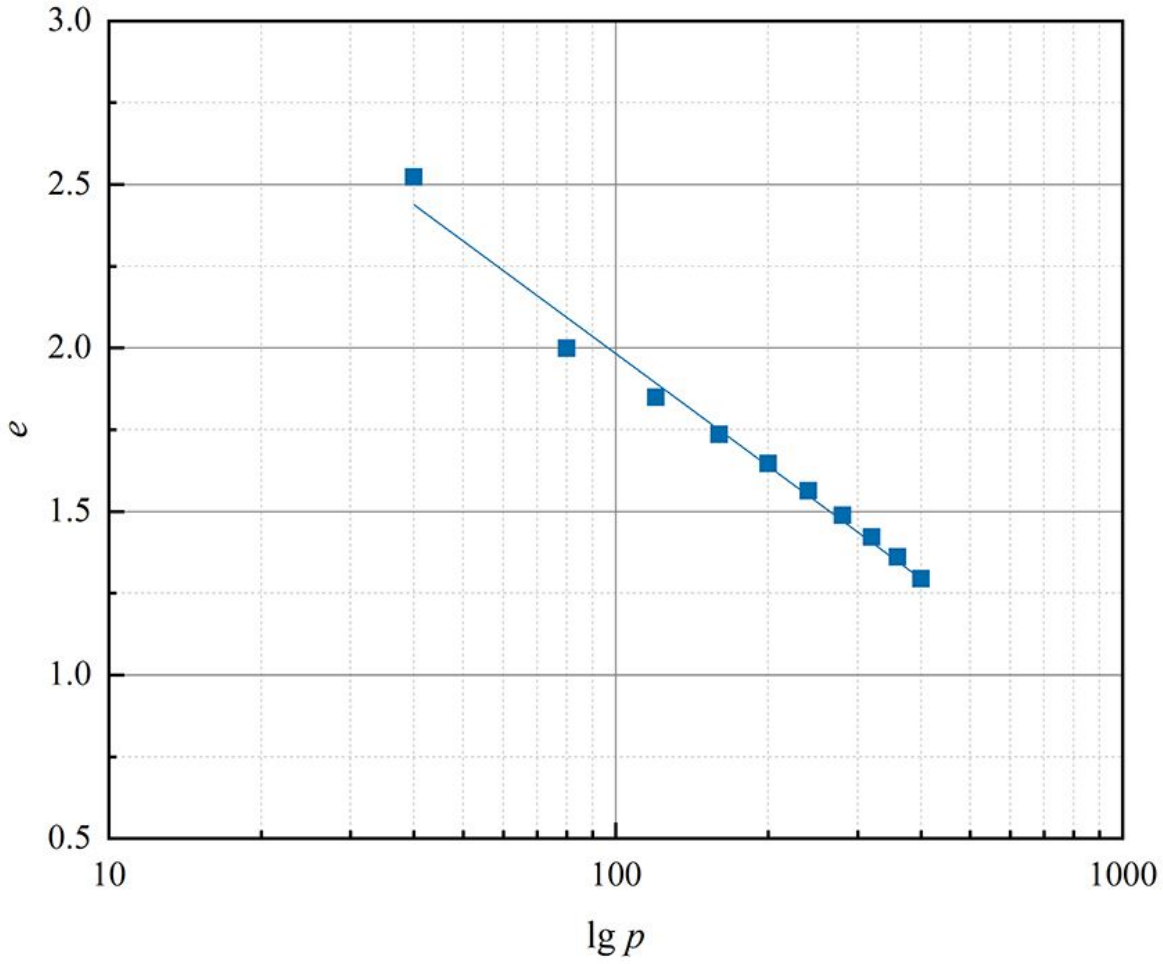

Figure 5

The relationship between the porosity ratio (e) and the logarithm of vertical pressure (lg p).

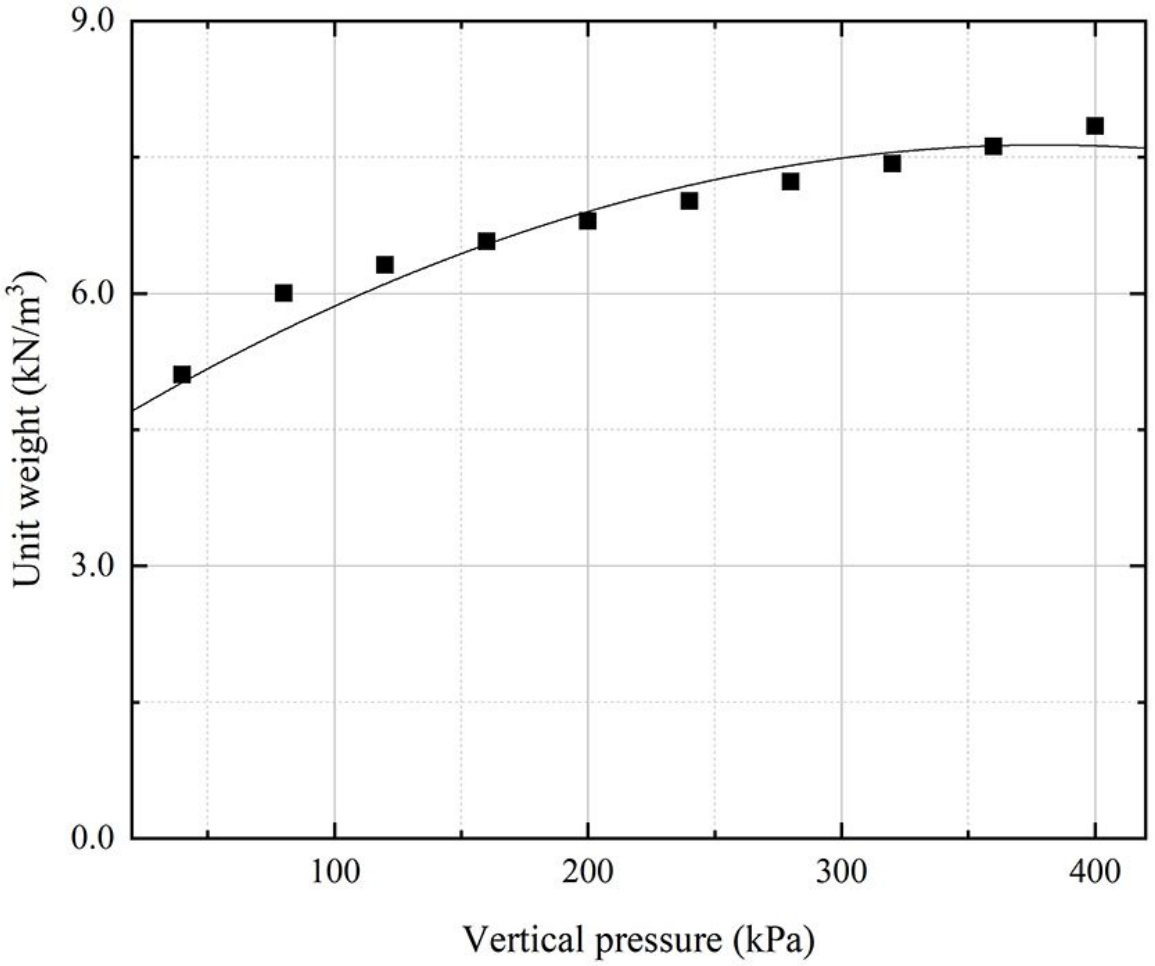

Figure 6

The relationship between the unit weight of the sample and the vertical pressure.

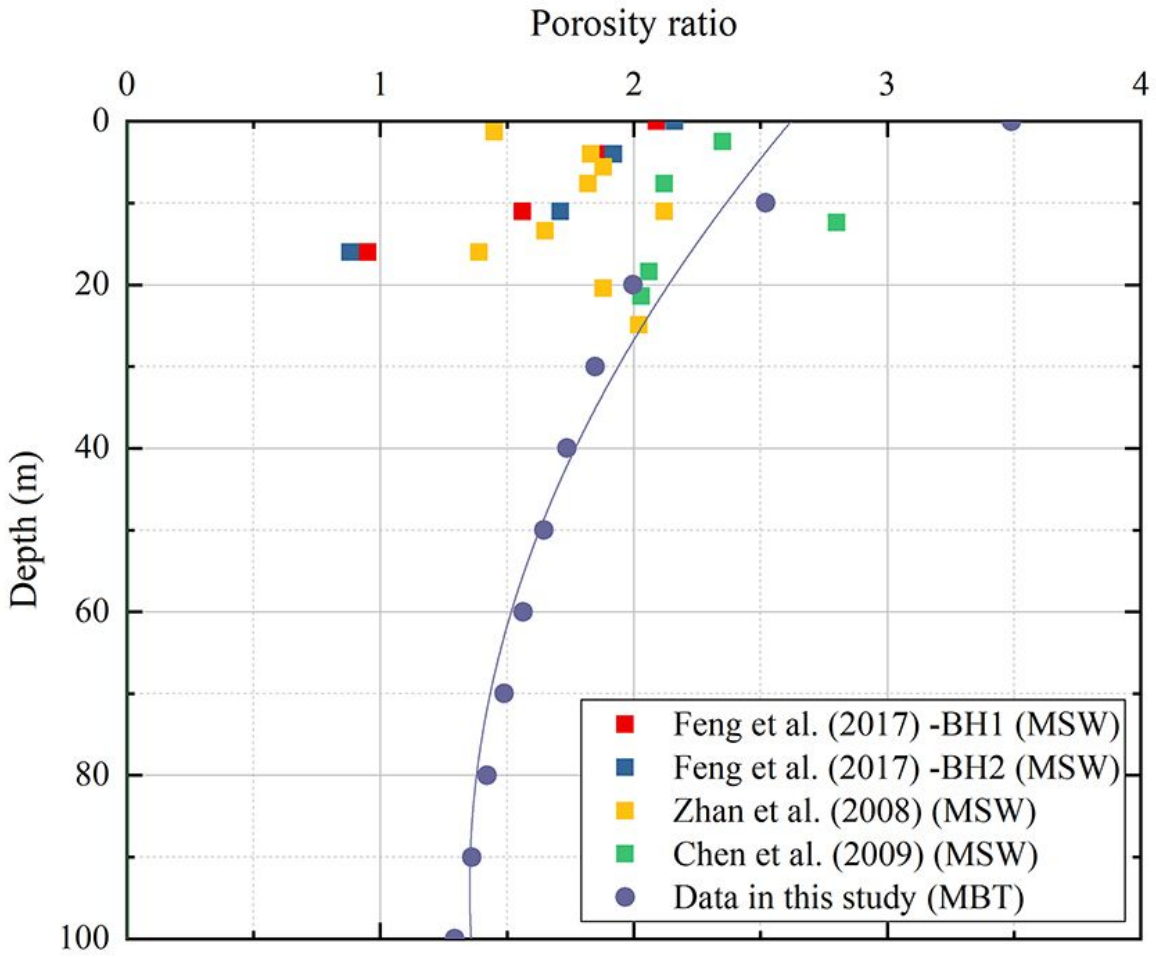

Figure 7

The porosity ratio of MSW and MBT waste varies with depth.

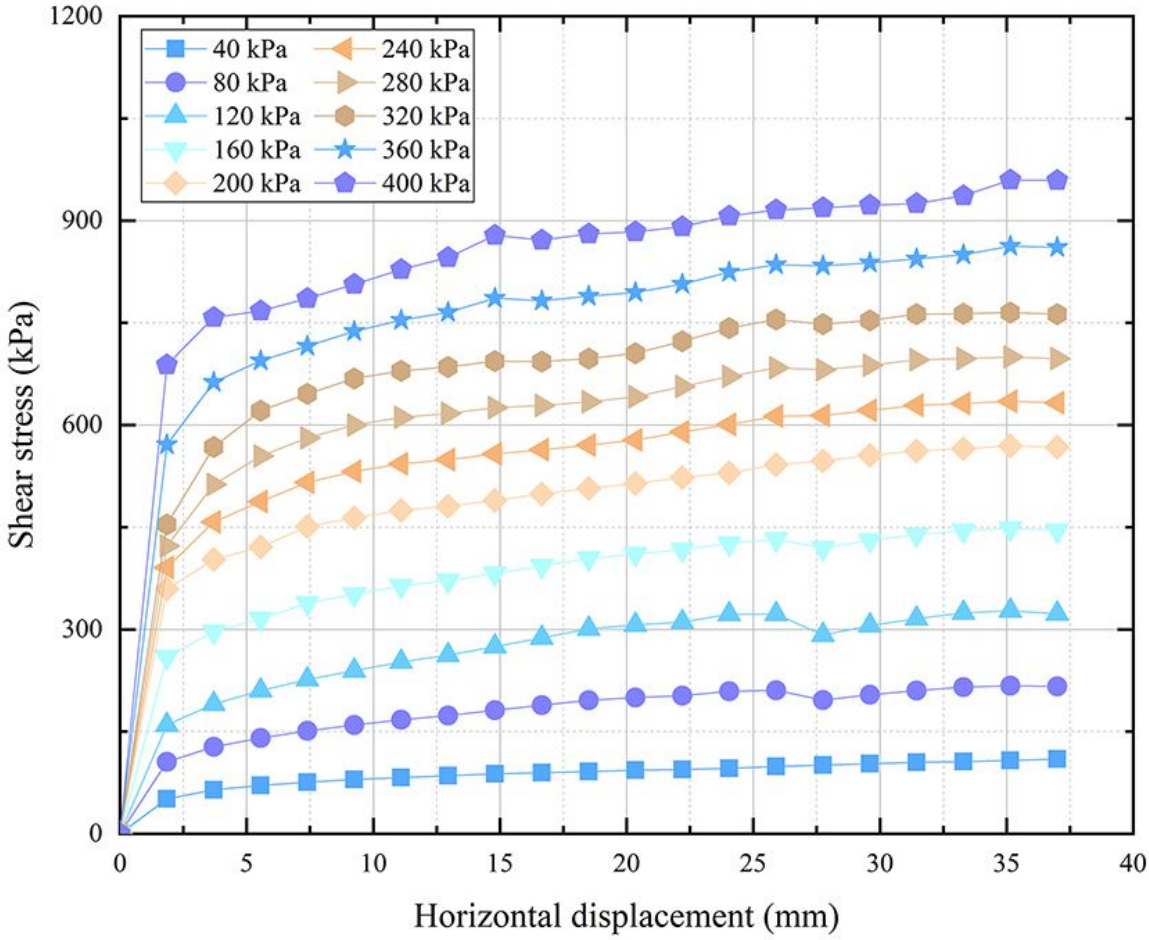

Figure 8

Shear stress-horizontal displacement graph (shearing rate is 5mm/min).

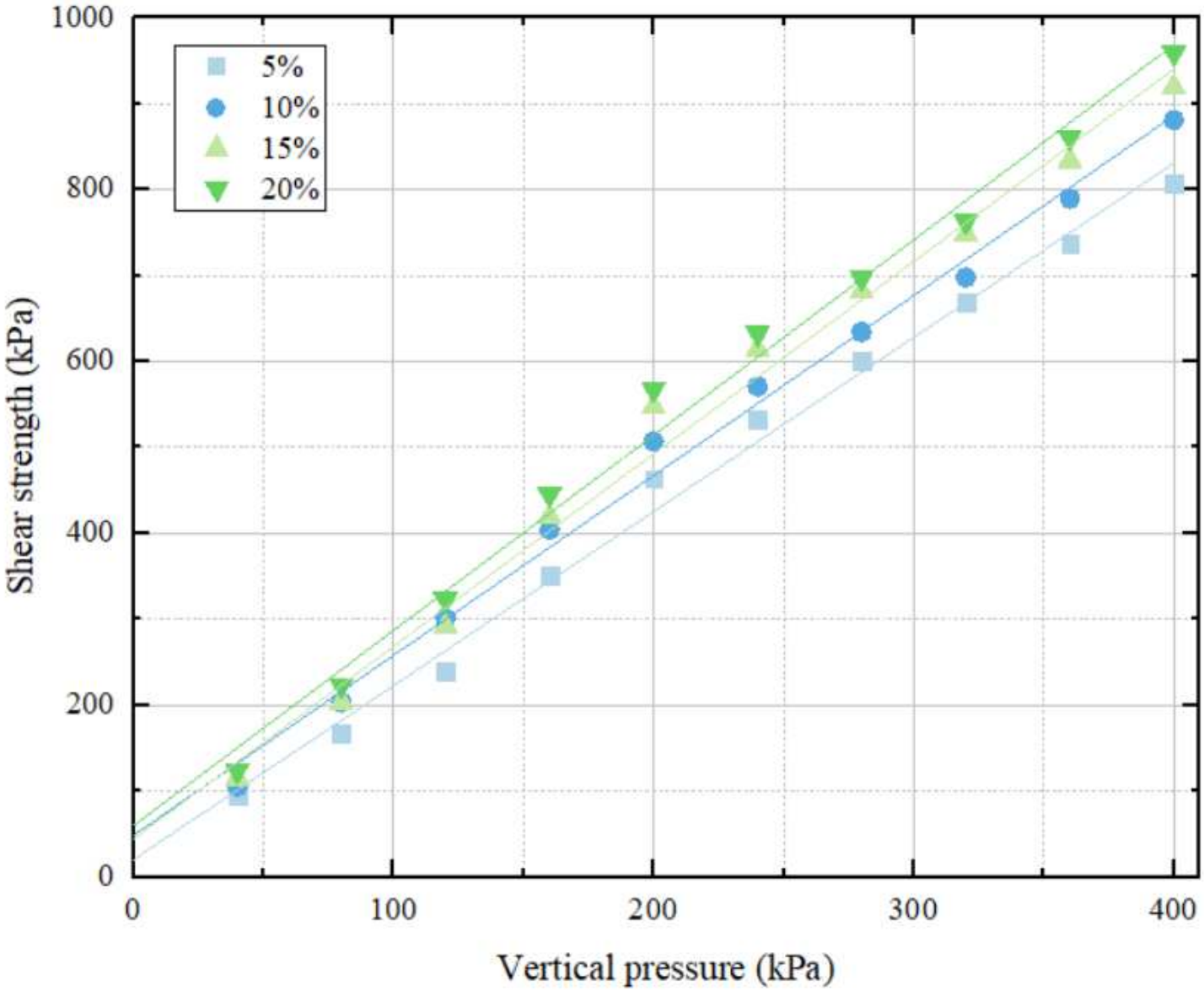

Figure 9

MBT waste shear strength envelope (shearing rate is 5mm/min).

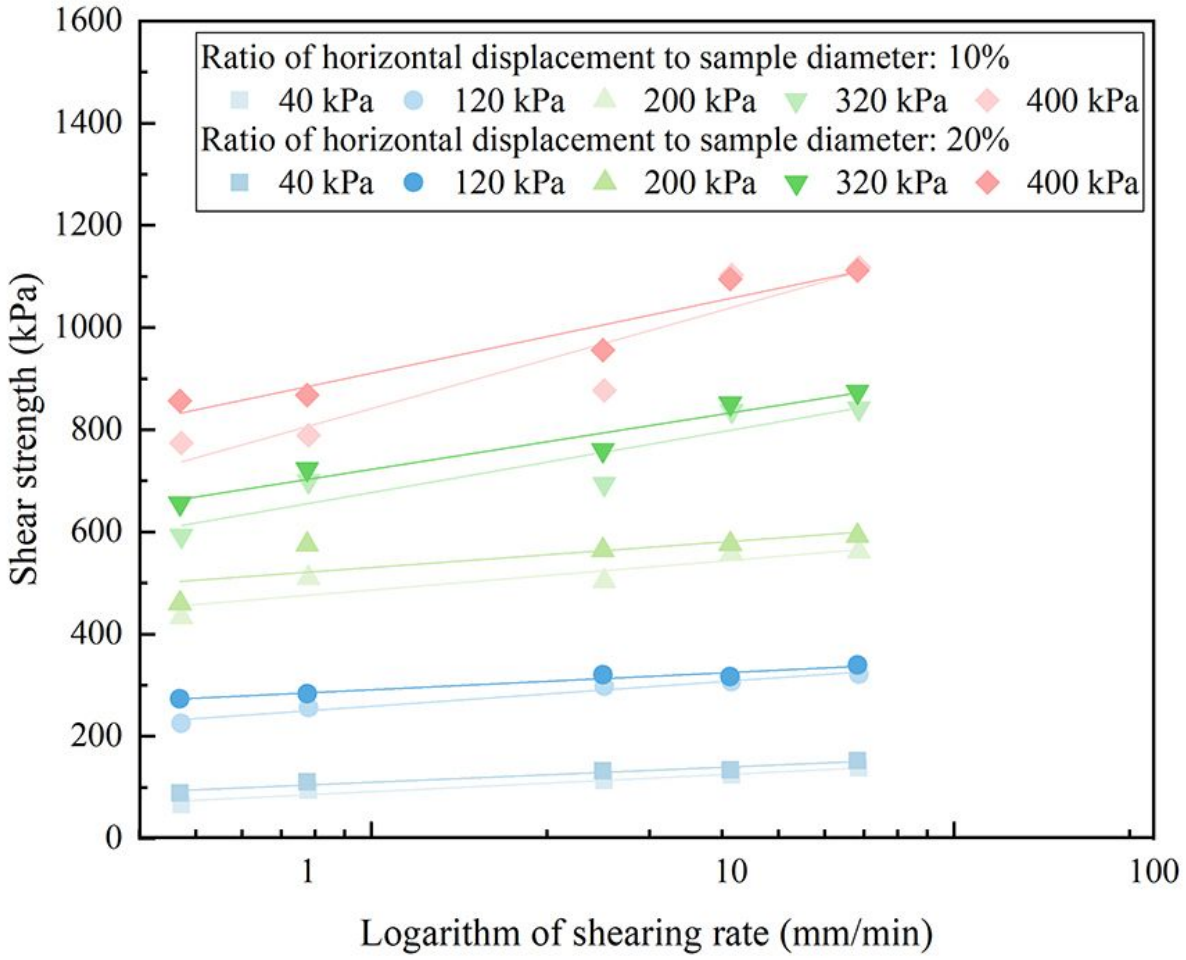

Figure 10

The relationship between shear strength and logarithm of shearing rate.

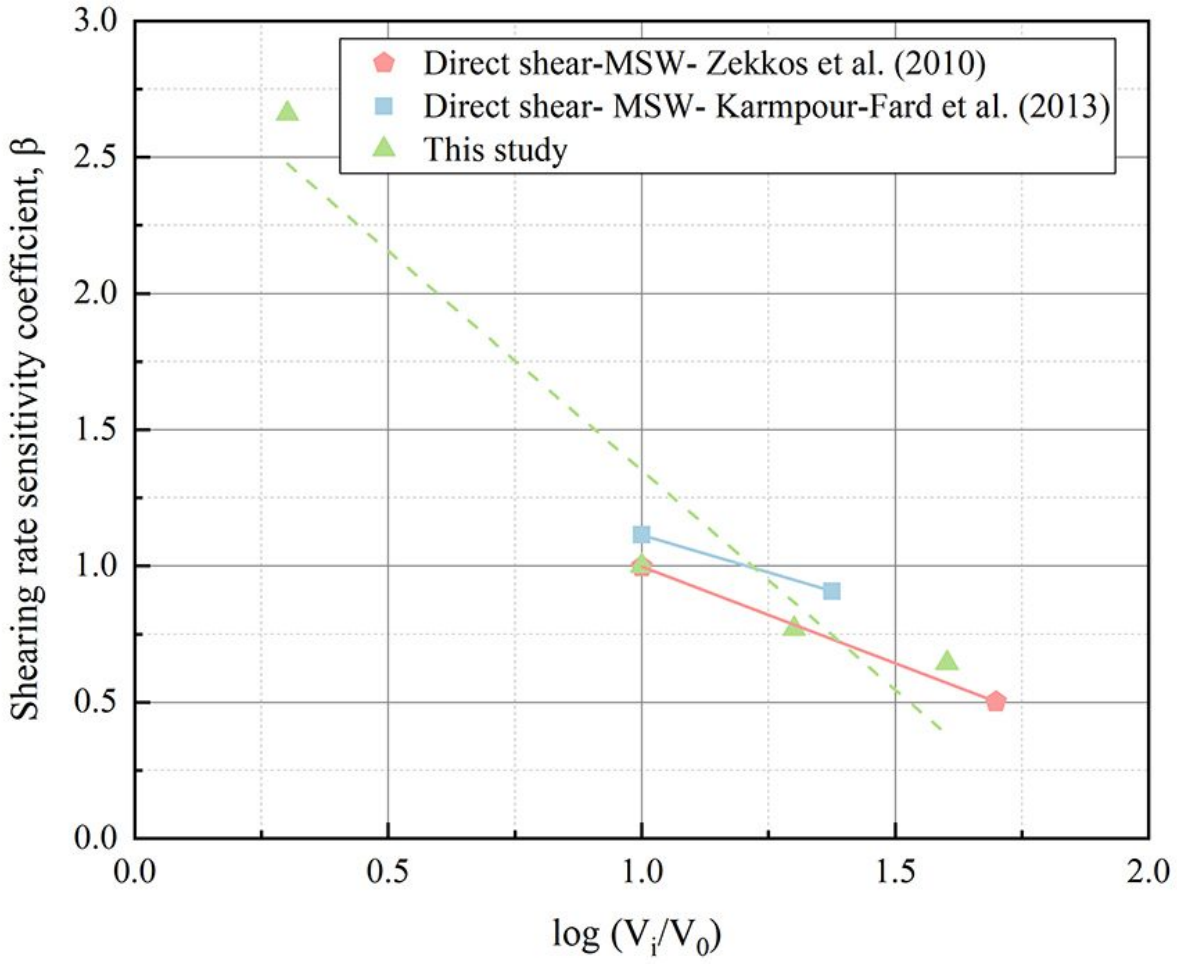

Figure 11

The shearing rate sensitivity coefficient of waste samples.

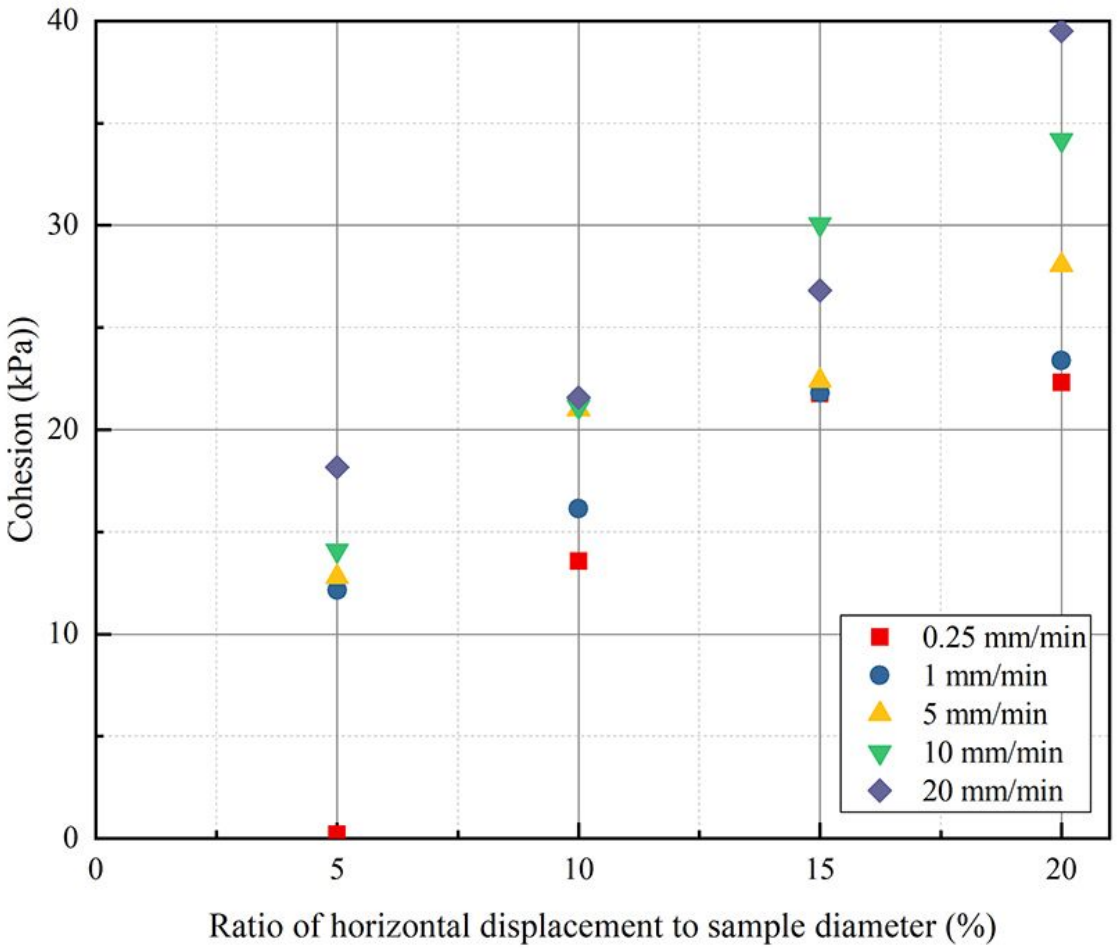

Figure 12

The relationship between cohesion and ratio of horizontal displacement to sample diameter.

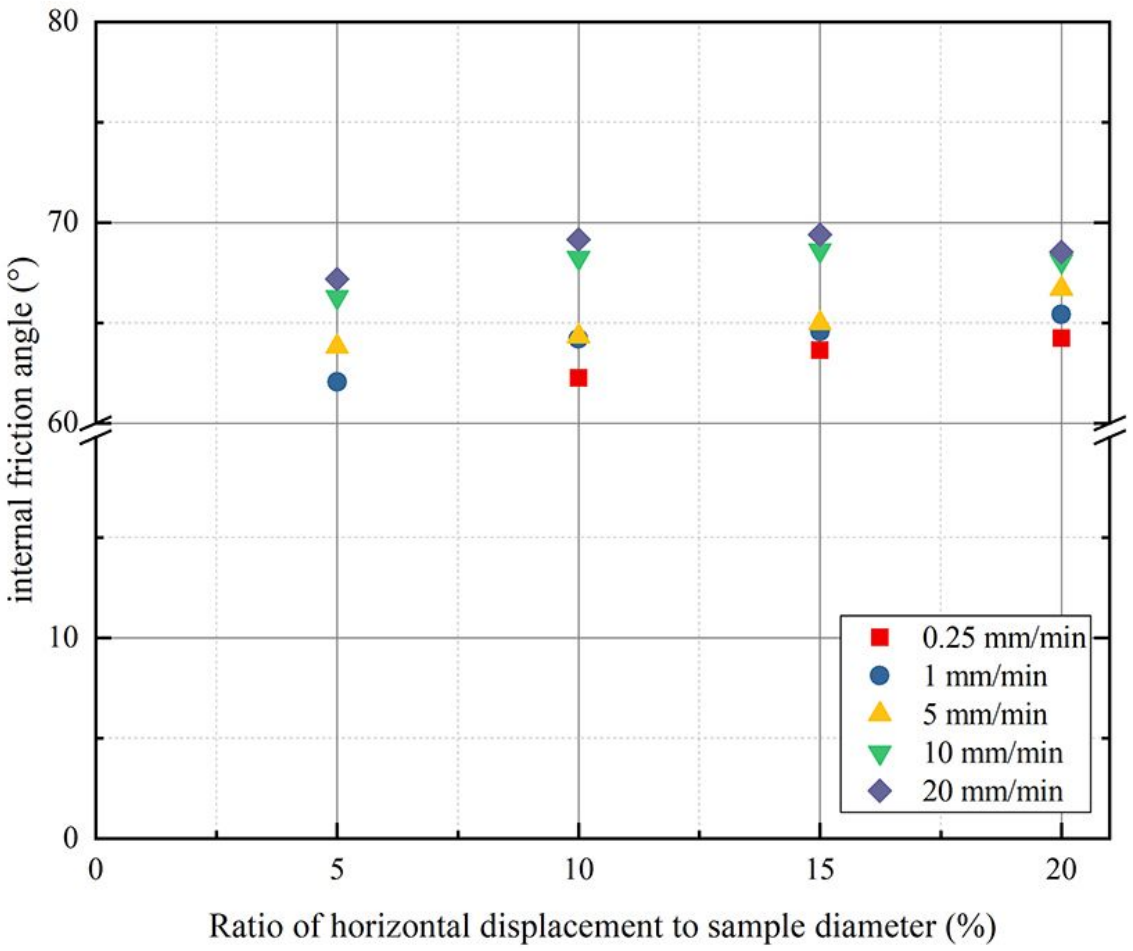

Figure 13

The relationship between internal friction angle and ratio of horizontal displacement to sample diameter.

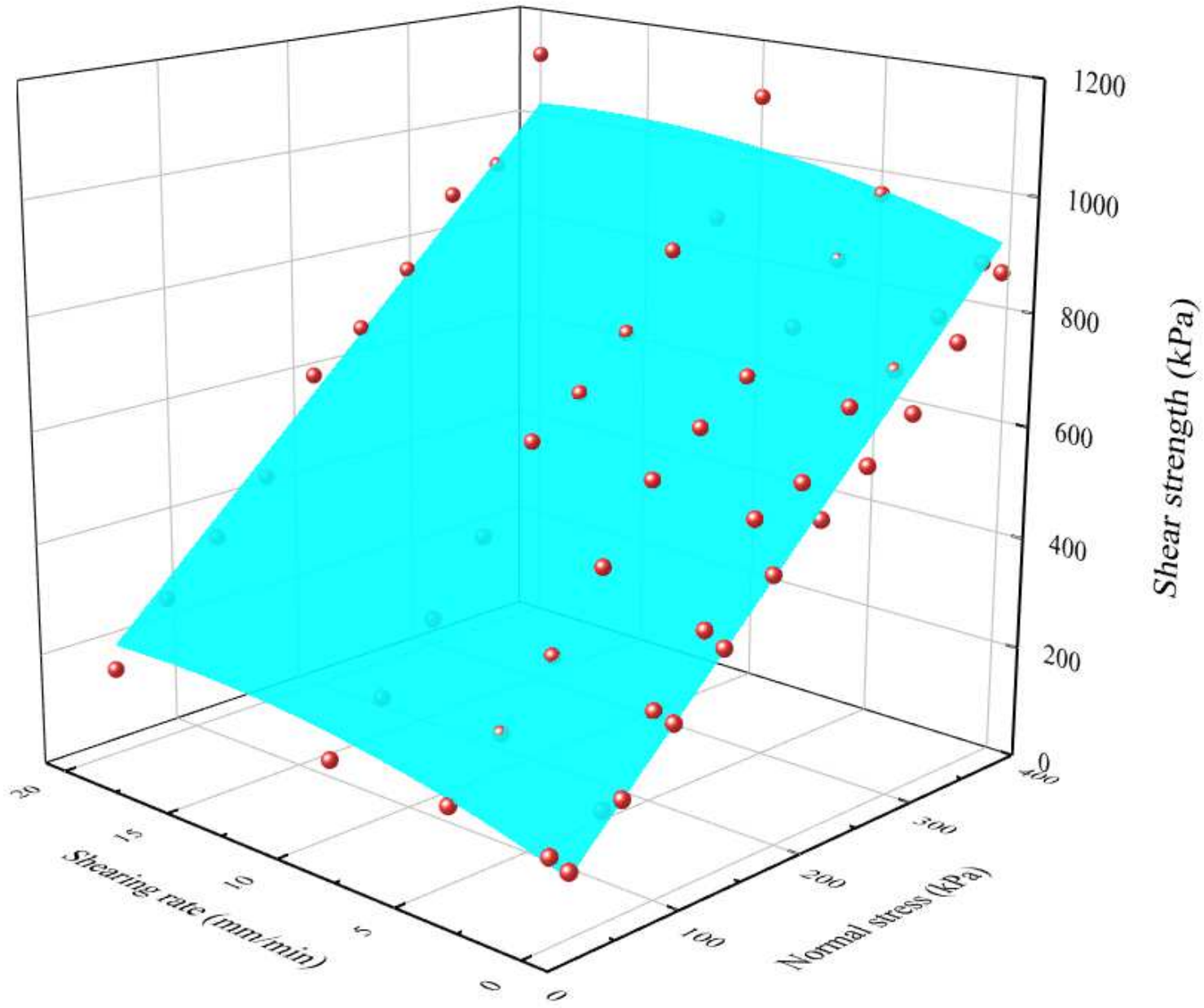

Figure 14

Shear strength fitting model.

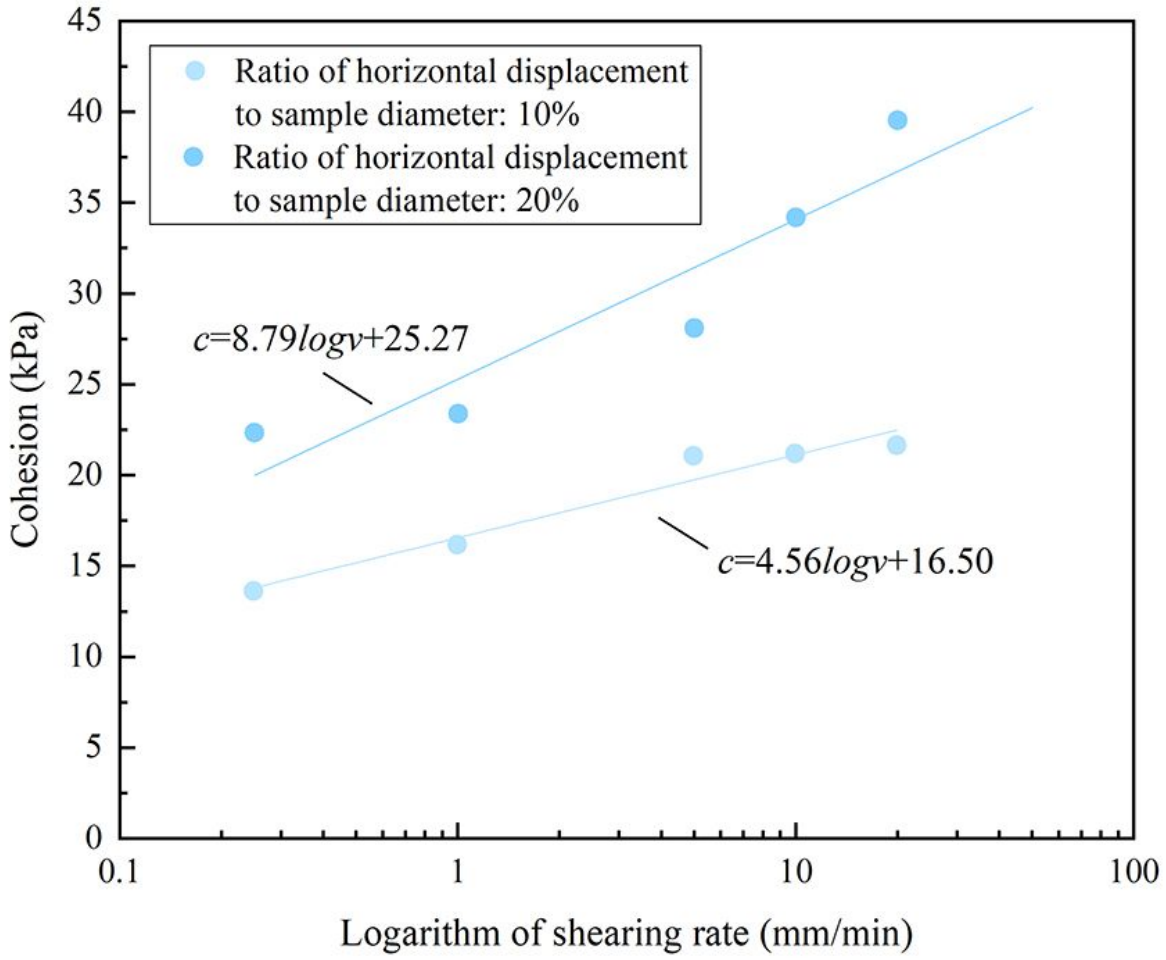

Figure 15

Relationship between cohesion and logarithm of shearing rate.

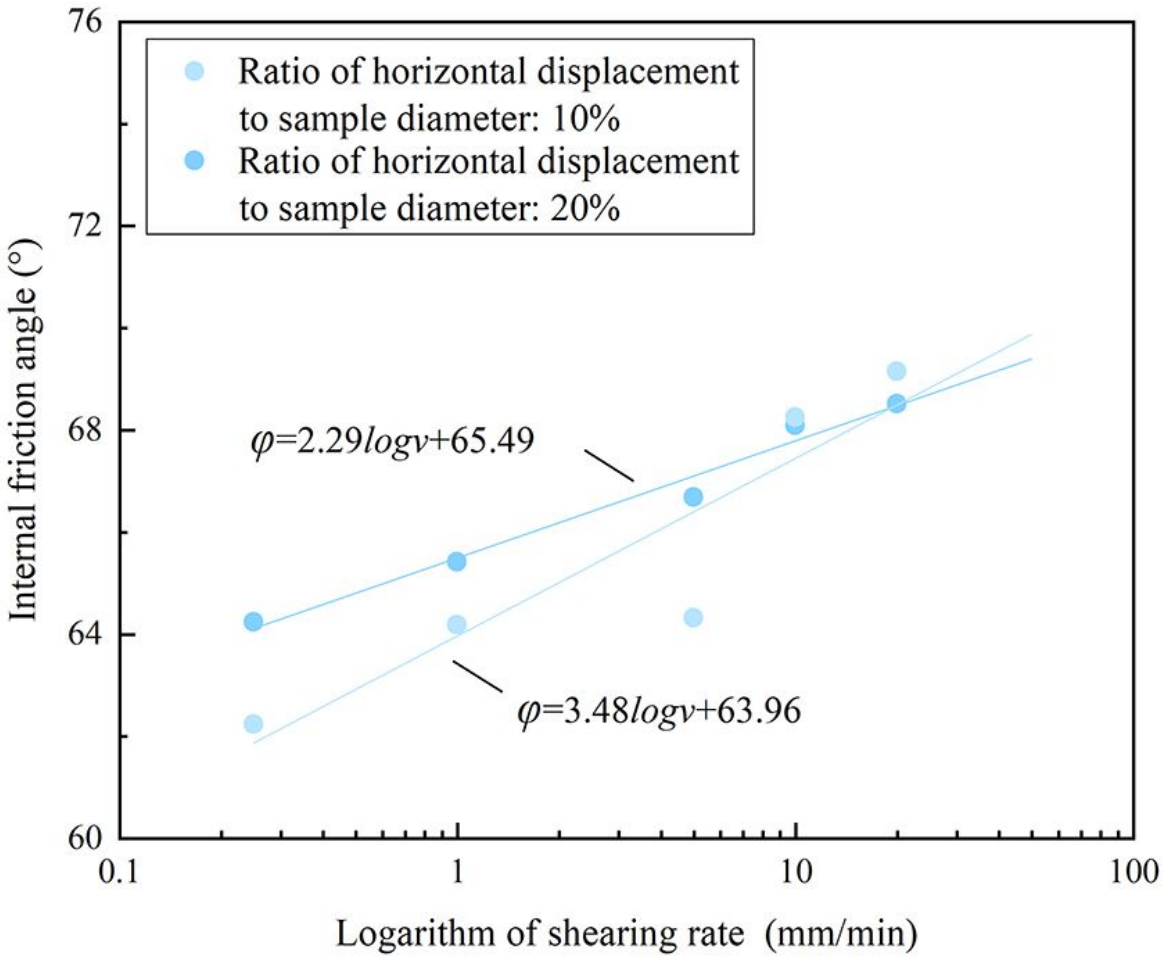

Figure 16

Relationship between internal friction angle and logarithm of shearing rate.

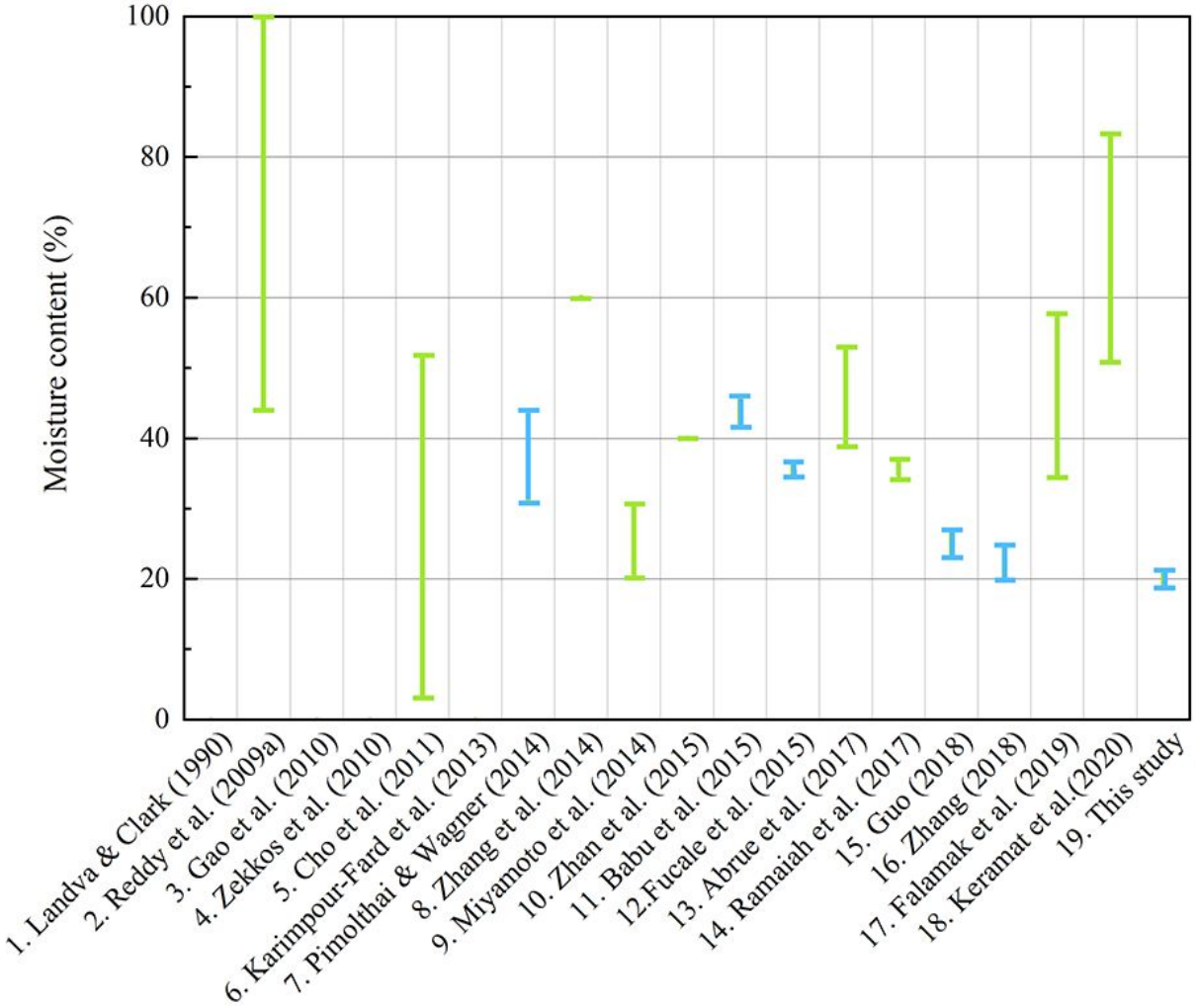

Figure 17

Moisture content of each reference sample (green - MSW, blue - MBT waste).

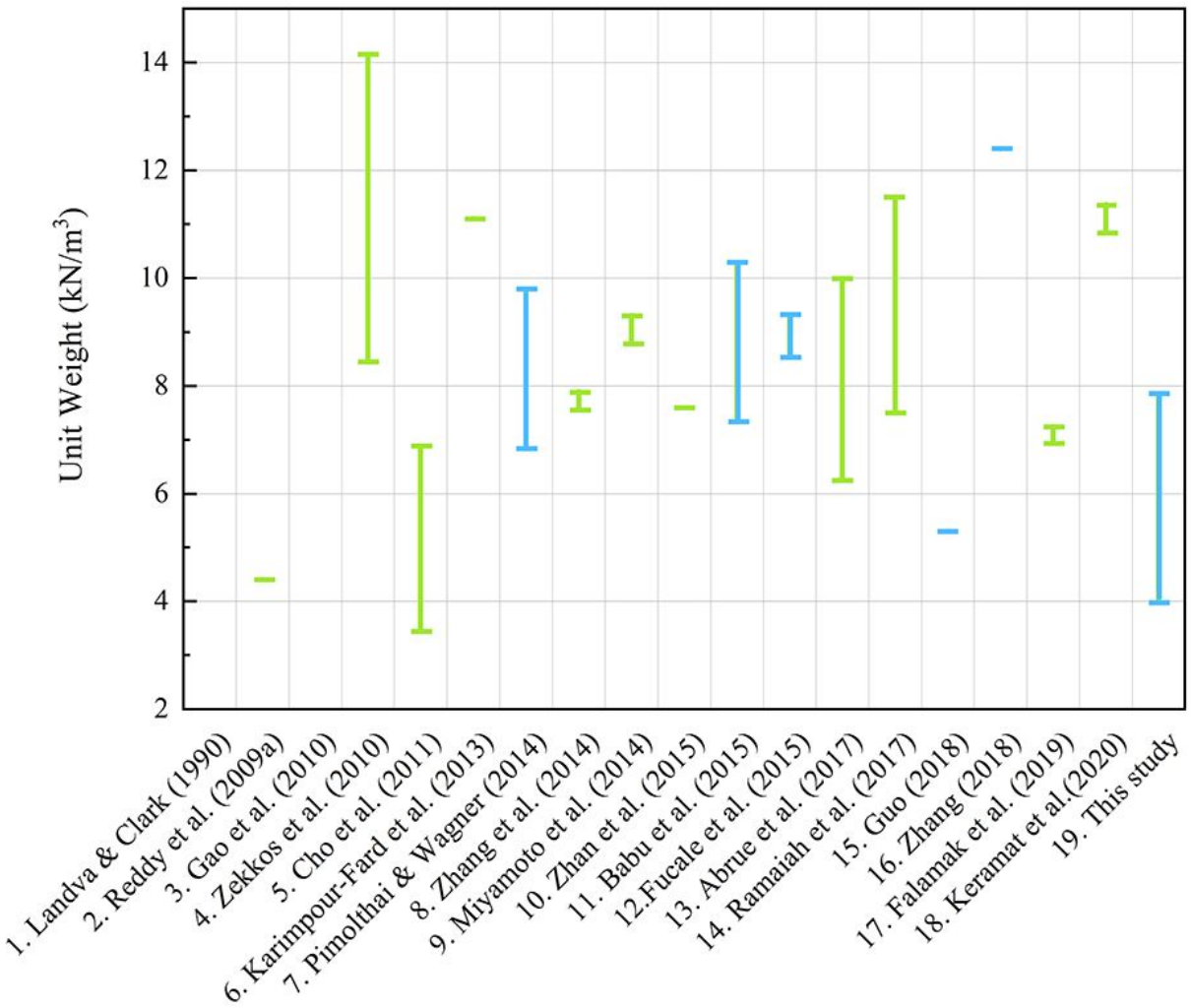

Figure 18

Unit weight of each reference sample (green - MSW, blue - MBT waste).

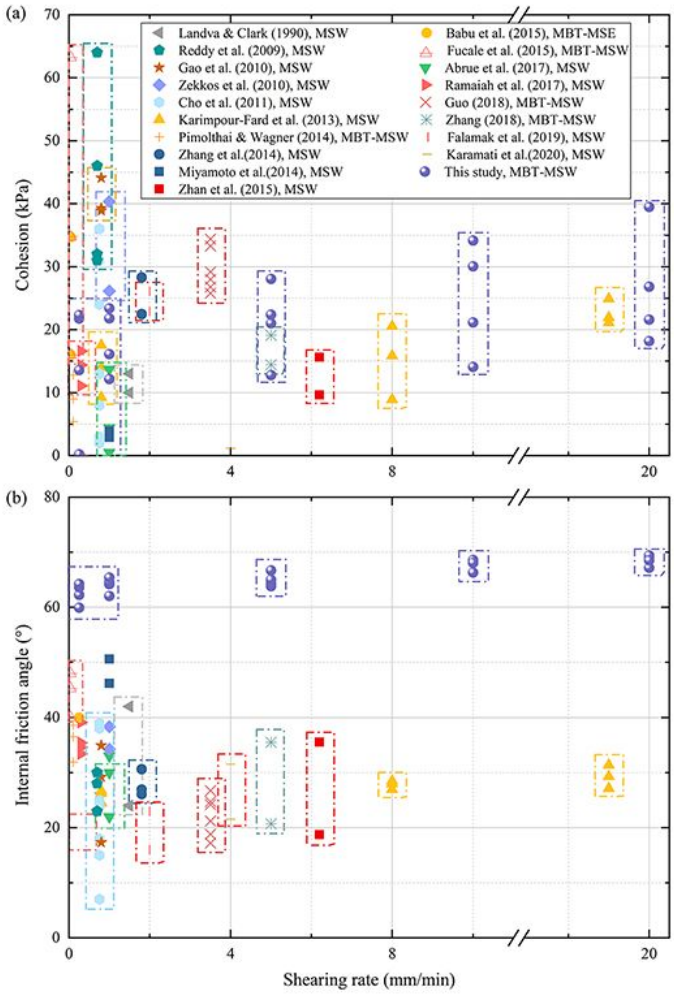

Figure 19

Comparison of shear strength parameters (a) the relationship between cohesion and shearing rate, (b) the relationship between internal friction angle and shearing rate.